

Vaccination against rubella and measles: quantitative investigations of different policies

BY R. M. ANDERSON

*Department of Pure and Applied Biology, Imperial College, London University,
London SW7 2BB, England*

AND R. M. MAY

Biology Department, Princeton University, Princeton, New Jersey 08544, U.S.A.

(Received 22 October 1982; accepted 25 November 1982)

SUMMARY

This paper uses relatively simple and deterministic mathematical models to examine the impact that different immunization policies have on the age-specific incidence of rubella and measles. Following earlier work by Knox (1980) and others, we show that immunization programmes can, under some circumstances, increase the total number of cases among older age groups; the implications for the overall incidence of measles encephalitis and of congenital rubella syndrome are examined, paying attention both to the eventual equilibrium and to the short-term effect in the first few decades after immunization is initiated. Throughout, we use data (from the U.K., and U.S.A. and other countries) both in the estimation of the epidemiological parameters in our models, and in comparison between theoretical predictions and observed facts. The conclusions defy brief summary and are set out at the end of the paper.

INTRODUCTION

Some years ago, in a commentary in the *American Journal of Epidemiology* Fox *et al.* (1971) argued that the planning of large-scale immunization programmes should be based on a full understanding of the principle of herd immunity. This principle rests on the belief that the chance of infection being acquired within a community is related, in some manner, to both the density of susceptibles and the density of infectious individuals. As shown by recent epidemiological studies of vaccinated populations, mass immunization apparently acts to reduce the average density of infectives and may have relatively little influence on the overall density of susceptibles (Fine & Clarkson, 1982). These observations are supported by theoretical studies which suggest that the average number of susceptibles will remain approximately constant in value, independent of the level of vaccine coverage, until the degree of herd immunity approaches a critical value above which the infection is unable to persist within the community (Anderson & May, 1982). Implicit in the principle of herd immunity is the assumption that protection of the individual may be achieved by the protection of the community as a whole.

Today the comments of Fox *et al.* (1971) appear as cogent as ever. Of relevance is the dramatic decline in reported cases of measles in the U.S.A. over the past few years under the pressure of intensive immunization coverage, and the recent resurgence of pertussis in the U.K. concomitant with a decline in rates of vaccine acceptance.

An important and sometimes little-appreciated consequence of mass immunization is its tendency to raise the average age at which an individual typically acquires an infection over that which pertained before mass vaccination; fewer individuals acquire infection, but those that do are on average older. Changes in the age distributions of reported cases of rubella and measles in the U.S.A. after the introduction of vaccination are good examples of this trend. As emphasized in an important paper by Knox (1980), such an increase in the average age at infection may, under certain circumstances, actually result in greater incidence of infection among older age classes of the community than was the case before vaccination. This observation, backed by the predictions of theoretical studies, has generated some concern over the wisdom of adopting mass immunization programmes against viral and bacterial infections whose effects are typically milder among children than among older people. Specifically, empirical observations suggest that the risk of serious disease arising from many common viral infections may increase with age: the incidences of encephalitis and meningitis as complications of viral infections, for example, are in general higher among adults than among children. A different, but related, concern arises if maternal infection during pregnancy is associated with risk of serious disease in the unborn infant; congenital rubella syndrome (CRS) is a good example of this phenomenon. In these circumstances, mass immunization may be of benefit to the community in diminishing the overall incidence of infection, but may be disadvantageous to individuals in the older, high risk, age classes (such as women in their childbearing years). In other words, protection of the individuals mainly at risk is not necessarily achieved by the protection of the community as a whole.

For infections like rubella, the considerations outlined above have led to the adoption of different vaccination policies by different countries. Some policies, such as that currently adopted in the USA, seek to immunize large numbers of children at a pre-school age, with the aim of reducing the overall rate at which the virus circulates within the community and thence the incidence of cases in women of childbearing age. Other policies, such as that currently adopted in the U.K., seek to encourage the acquisition of immunity by natural infection during early childhood, by vaccinating only those individuals who will become at risk (i.e. girls) just before they enter the high-risk age classes.

There remain, however, many questions of a quantitative kind about the relative merits of the different approaches. What levels of immunization coverage of young children must be achieved in order significantly to reduce the incidence of rubella in women of child-bearing age? Under what circumstances does the U.K. policy do better than the U.S.A. one in reducing disease incidence? How is the temporal behaviour of an infection within a community influenced by different vaccination programmes?

These and other related questions have recently been examined by Knox (1980), Dietz (1981), Hethcote (1983) and Cvjetanovic, Dixon & Grab (1982). Three of these

studies are concerned with vaccination against rubella: Knox (1980) examines the long-term effect on disease incidence of various vaccination policies, and also uses computer models to explore the short-term, 'transient' effects attendant upon the initiation of vaccination; Dietz (1981) and Hethcote (1983) give analytic treatments of long-term effects, taking some account of economic cost–benefit considerations. Although these studies are seminal, they concentrate on formal results and do not present any explicit comparison between theoretical results and observed epidemiological data. Cvjetanovic *et al.* (1982) examine measles, and give results for a complex study of various vaccination policies, based on computer simulations; these authors omit description of some important details of their methods and assumptions (it is not clear, for example, how they estimate the rate of infection in communities under different levels of vaccination uptake). The simulation models of both Knox and Cvjetanovic and colleagues are complex in structure; this has the advantage that the models can embrace more biological detail, and the associated disadvantage that it is not always clear how particular conclusions follow from particular initial assumptions.

The present study attempts to extend the work described above. Our emphasis is on the impact that various vaccination policies may have on the incidences of CRS and of measles encephalitis. Using simple deterministic models for infections in age-structured human populations, we examine the way the incidence of disease changes, both in the short and in the long term, following the inauguration of a vaccination programme. We particularly emphasize: (i) explicit enunciation of the assumptions incorporated in the model; (ii) of empirical data to estimate the epidemiological parameters in the models; and (iii) comparison between the predictions of the model and observed facts. Our focus is on the impact of vaccination on the incidence of disease; we do not consider economic cost–benefit aspects of differing control policies.

The paper is organized as follows. The first section discusses various basic concepts relevant to the dynamics of directly transmitted diseases within human communities; this section outlines the structure of the model employed in later sections. The second and third sections examine the impact of vaccination on the incidence of CRS. They consider, respectively, observed epidemiological patterns and the predictions of our theoretical analyses. The fourth and fifth sections are similar to the second the third, but examine the impact of vaccination on the incidence of measles encephalitis. The final two sections discuss, respectively, future research needs and the conclusions of our analyses. Mathematical details are kept to a minimum in the main text and formal developments are dealt with in appendices.

We have made an effort to write the paper so that it is accessible at three levels. Those who are unhappy with mathematics can skip the lengthy first section, and go directly to the empirical and result-oriented later sections; this choice has the drawback that the model itself (with all its shortcomings) must be taken on faith, which is always dangerous. All the essential elements of our study can be grasped by reading the entire main text of the paper, omitting the appendices. At a third level, the appendices are there for those who enjoy the details, or wish to repeat, modify or extend the calculations.

METHODS AND GENERAL CONCEPTS

Compartmental models

Compartmental mathematical models are widely used to study the dynamics of viral, bacterial and many protozoan infections that are directly transmitted in human populations. These models are based on the assumption that the human community can be divided into a series of compartments containing, for example, susceptible, infected but not infectious, infectious, and immune individuals. Models of this type form the template from which much of the mathematical literature concerned with epidemic and endemic phenomena is created (Kermack & McKendrick, 1927; Soper, 1929; Bailey, 1975; Hoppensteadt, 1975; Dietz, 1976; Yorke *et al.* 1979; Anderson & May, 1982).

Our analysis of the impact of vaccination on the population dynamics of measles and rubella is based upon a compartmental model with age structure. We begin by defining a fairly general model in which the numbers of individuals of age a , at time t , who are susceptible, infected but not infectious, infectious, and immune are denoted by the variables $X(a, t)$, $H(a, t)$, $Y(a, t)$ and $Z(a, t)$, respectively. We assume that the individuals are subject to an age-dependent mortality rate of $\mu(a)$ in age class a , and that new susceptibles enter the population by birth at a net rate $B(\bar{N})$ which is some function of total community size $\bar{N}(t)$ at time t . We denote the total number of susceptible, latent, infectious, and immune individuals at time t as $\bar{X}(t)$, $\bar{H}(t)$, $\bar{Y}(t)$ and $\bar{Z}(t)$, respectively; these aggregated quantities are derived by summing or integrating over all age classes, so that, for example,

$$\bar{X}(t) = \int_0^{\infty} X(a, t) da, \quad (1)$$

and so on. The total population at time t is, of course

$$\bar{N}(t) = \bar{X}(t) + \bar{H}(t) + \bar{Y}(t) + \bar{Z}(t). \quad (2)$$

Individuals are assumed to leave the latent class to join the infectious class at an age-independent rate σ ; the average duration of stay in the infected but not infectious state (the *latent period*) is thus $1/\sigma$. Similarly, we assume that the rate of recovery, γ , from the infectious class to join the immune class is age-independent; the average infectious period is then $1/\gamma$. Susceptibles of age a are assumed to acquire the infection at a per capita rate $\lambda(a, \bar{Y}(t))$; λ is the so-called 'force of infection', which at time t is some function of the total number of infectious individuals within the community. Finally, for the sake of generality, we assume that infectious individuals (as a consequence of infection) are subject to an additional mortality rate, $\alpha(a)$ at age a , over and above the natural mortality rate $\mu(a)$.

These assumptions may be translated into a set of first-order nonlinear partial differential equations, which describe the rates of change of X , H , Y , and Z with respect both to age a and to time t :

$$\frac{\partial X(a, t)}{\partial t} + \frac{\partial X(a, t)}{\partial a} = -[\mu(a) + \lambda(a, \bar{Y}(t))] X(a, t) \quad (3)$$

$$\frac{\partial H(a, t)}{\partial t} + \frac{\partial H(a, t)}{\partial a} = \lambda(a, \bar{Y}(t)) X(a, t) - [\mu(a) + \sigma] H(a, t) \quad (4)$$

$$\frac{\partial Y(a, t)}{\partial t} + \frac{\partial Y(a, t)}{\partial a} = \sigma H(a, t) - [\mu(a) + \alpha(a) + \gamma] Y(a, t) \quad (5)$$

$$\frac{\partial Z(a, t)}{\partial t} + \frac{\partial Z(a, t)}{\partial a} = \gamma Y(a, t) - \mu(a) Z(a, t). \quad (6)$$

These equations may look messy, but they say intuitively comprehensible things. The left-hand expressions describe, for example, the change in the number of susceptibles; the explicit changes with respect to time and to age have a symmetrical appearance ($\partial/\partial t + \partial/\partial a$) essentially for the commonsense reason that in one year people grow one year older. On the right-hand side, susceptibles appear by births (as described by the boundary conditions; see below), and are lost by deaths or by acquiring infection. This latter process carries them to the latent stage, whence they are lost to the fully infectious class (or they may die). Infectious individuals in turn either die (from the disease or other causes), or recover to the immune class. Immunity is here assumed to be lifelong, so that death is the only exit from this class (loss of immunity could be included by a term that carries individuals from the immune class back into the susceptible one). It will often be more biologically accurate to treat individuals as spending a definite period in the latent or infectious state, rather than moving out of these states at a constant rate (σ and γ , respectively); a variety of studies suggest, however, that such refinements will not significantly affect the kind of conclusions we draw below (Hethcote & Tudor, 1980; Grossman, 1980; Waltman, 1974; Hoppensteadt, 1975; Aron, 1983).

The partial differential equations (3)–(6) describe the system, provided that initial and boundary conditions are specified. Usually one such condition is determined by giving all the age distributions, at time $t = 0$; that is, by specifying $X(a, 0)$, $H(a, 0)$, $Y(a, 0)$, $Z(a, 0)$, for all a at $t = 0$. The other boundary condition typically follows from the assumption that all newborn individuals are susceptible to infection, so that $X(0, t) = N(0, t)$ and $H(0, t) = Y(0, t) = Z(0, t) = 0$, for all t at $a = 0$ (here $N(0, t)$ is the number of newborn individuals, the total population of age $a = 0$ at time t ; total number of births will depend in some defined way on the total number of individuals in various age classes). This second condition is easily modified to take account of the biological fact that newborn infants may be protected from infection by maternal antibodies for a short period (commonly of the order of 3 to 9 months); this issue is discussed in more detail below.

The model defined in equations (3)–(6) is couched in fairly general terms, and it may be modified to incorporate various assumptions about programmes of disease control (such as mass immunization). For example, vaccination of the susceptible class at an age-dependent per capita rate $c(a)$ may be represented by including a loss term $c(a) X(a, t)$ in equation (3) for the susceptibles and a gain term of identical magnitude in equation (6) for the immune class.

For a specified infection in a particular human community, the model defined by equations (3)–(6) may be solved by numerical methods, to generate time-dependent solutions for the numbers of individuals of age a in each of the four classes, X , H , Y , and Z , at time t . To do this, however, we need to know all the age-dependent ($\mu(a)$, $\alpha(a)$, $\lambda(a, \bar{Y}(t))$) and age-independent ($B(\bar{N})$, σ , γ) rate parameters that control the movement of individuals from one compartment of the model to another. For some viral infections, such as measles and rubella in developed countries, this type of detailed quantitative information is sometimes

available. Before proceeding to such detailed studies, however, we pause to survey some general insights that come from considering the equilibrium states (the *statics*) of various limiting versions of the general model. These ideas can help us to understand the complicated temporal behaviour (the *dynamics*) of the more general model.

Basic concepts

We first discuss ways in which the 'force of infection', λ , may be evaluated. One widely employed assumption in mathematical epidemiology is that the net rate of acquisition of infection within the population is proportional to the product of the density of susceptibles, \bar{X} , times the density of infectives, \bar{Y} ; that is, infections appear at the rate $\beta\bar{X}\bar{Y}$, where β is a 'transmission coefficient'. This assumption is sometimes called the 'mass action' principle (in obvious analogy with the processes deriving from binary collisions between atoms in an ideal gas), and it rests in part on the assumption that the population is 'homogeneously mixed' (with local groupings in families or schools all averaged out). The coefficient β here has two components, one representing the average frequency of contact between susceptibles and infectives, and the other denoting the likelihood that a contact actually results in transmission. Under this assumption the per capita force of infection at time t , $\lambda(t)$, is given by

$$\lambda(t) = \beta \int_0^{\infty} Y(a, t) da. \quad (7)$$

Although all the other parameters in the general model (μ , σ , λ , α) may be measured, any direct estimate of the transmission parameter β is likely to be quite hopeless in view of the diversity of factors compounded in it.

The parameter λ may, however, in equilibrium situations often be determined directly; this possibility is pursued further below, and in Appendix 2. In order to discuss equilibrium circumstances, we must first restrict the generality of equations (3)–(6) in two ways. First, we follow the almost universal practice of taking the total community size to be approximately constant, so that the net input of susceptibles by births roughly balances the net loss due to deaths; things are substantially more complicated if the total size of the population is itself rapidly changing. Second, we follow the even more invariable practice of assuming the infection is not a significant cause of mortality (i.e. $\alpha = 0$). It is then a relatively straightforward matter to obtain the equilibrium versions of equations (3)–(6) by dropping all dependence on t (which includes putting all the partial derivatives $\partial/\partial t = 0$); this leads to a set of first-order ordinary differential equations for $X(a)$, $H(a)$, $Y(a)$ and $Z(a)$. As discussed more fully in Appendix 1, explicit expressions for these equilibrium age-distributions may be obtained. In particular, at equilibrium the fraction of all individuals in age class a that are susceptible, $x(a) \equiv X(a)/N(a)$, is given by

$$x(a) = \exp\left(-\int_0^a \lambda(s) ds\right). \quad (8)$$

Thus if we have serological or other information about the age-specific susceptibility patterns, we can deduce the age-specific force of infection, $\lambda(a)$. Notice also that,

if λ is taken to be a constant, it is simply the inverse of the average age at first infection, A (so that λ can be inferred directly from knowledge of A):

$$A \equiv \int_0^{\infty} x(a) da = 1/\lambda. \quad (9)$$

These questions are pursued in detail in Appendix 2.

It is worth emphasizing that, if λ is estimated directly, the overall rate of acquisition of infection, $\lambda\bar{X}$, is only explicitly assumed to be proportional to the density of susceptibles, \bar{X} . This may be christened the assumption of 'weak homogeneous mixing', in contrast to the 'strong homogeneous mixing' assumption that this rate is proportional both to \bar{X} and to \bar{Y} , $\beta\bar{X}\bar{Y}$. It seems to us more likely to be true that the net rate of acquisition of new infections is proportional to the density of susceptibles, \bar{X} , than that it is proportional to the density of infectives, \bar{Y} ; doubling the number of susceptibles in a school is arguably more likely to double the net infection rate than is doubling the number of infectious individuals. In what follows, we will try to distinguish between tests of the theory that corroborate the usual (strong) 'homogeneous mixing' assumption from those that corroborate the 'weak homogeneous mixing' one.

The approach to estimating λ embodied in equations (8) and (9) is pretty much confined to equilibrium situations. Once the numbers of susceptible, latent, infectious, and immune individuals are changing in time, in response to some perturbation (such as a vaccination programme), we need to make some assumption about the way such changes will affect $\lambda(t)$: the simplest such assumption is that of (strong) homogeneous mixing.

In much of what follows, we deal with the total number of susceptible, latent, infectious, and immune individuals ($\bar{X}(t)$, $\bar{H}(t)$, $\bar{Y}(t)$ and $\bar{Z}(t)$, respectively) rather than with the age-structured details. These quantities are obtained from equation (1) and its relatives; they obey a set of first-order ordinary differential equations which may be derived by integration over all ages a in equations (3)–(6). These results are discussed in Appendix 1.

We now take up a series of detailed points pertaining to estimation of the various epidemiological and demographic parameters.

Human mortality

Most mathematical studies of the dynamics of viral (and bacterial and protozoan) infections in human communities assume that the death rate of individuals within the population is constant and independent of age: $\mu = \text{constant}$ (see, for example, Bailey, 1975; Dietz, 1975). This is done largely because it makes the mathematics easier and more elegant, rather than because real populations have age-independent death rates. As we see below, when a more realistic expression is used for $\mu(a)$ most epidemiological results are altered, albeit in a marginal way (rather than being qualitatively changed).

Fig. 1 displays the actual age-specific survivorship curve for the population of England and Wales (both females and males) in 1977; the average life expectancy within this population was approximately 75 years. This pattern is typical of those observed in many developed countries.

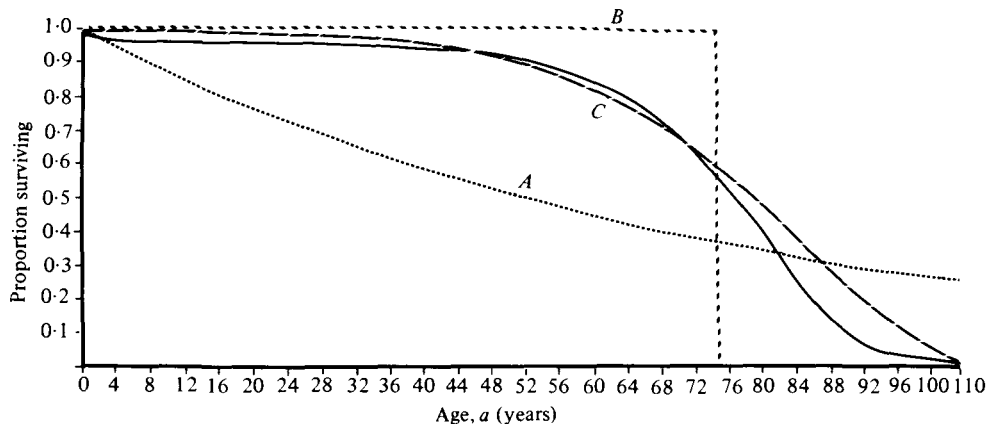


Fig. 1. The solid line records the age-dependent survival characteristics of females and males in England and Wales in 1977 (data from the Registrar General's Statistical Review for 1977). The age-specific mortality rate, $\mu(a)$, is the logarithmic derivative of this curve with respect to age a . Average life expectancy from birth, L , is 75 years. The dashed and dotted lines show the fits of three different survival models to this data. Survival curve type A is an exponential decay function with a constant age-independent death rate, μ , with value $\mu = 1/75 \text{ yr}^{-1}$. Survival curve type B is a step function model in which the death rate is assumed to be zero up to age 75 years and infinity thereafter. Survival curve type C is a Gompertz function which assumes that the death rate $\mu(a)$ rises exponentially with age where $\mu(a) = \bar{\alpha} \exp(-\bar{\gamma}a)$ with $\bar{\alpha} = 0.28 \times 10^{-3}$ and $\bar{\gamma} = 0.64 \times 10^{-1}$.

Fig. 1 also shows the fit between the facts and three different survival models (each of which assumed that life expectancy is $L = 75$ years). Curve (a) (*survival type A*) is an exponential decay curve with a constant, age-independent mortality rate μ set at $1/75 \text{ yr}^{-1}$. Curve (b) (*survival type B*) is a step function in which the mortality rate μ is assumed to be zero up to age $L = 75$ and infinite thereafter; everyone lives to exactly age L and then obligingly dies. Curve (c) (*survival type C*) is a Gompertz function in which the death rate is assumed to increase exponentially with age. A point to note in Fig. 1 is that a survival type A assumption is a poor reflexion of the observed numbers of children in different age classes, so that it is likely to give a relatively poor description of infections that predominate among children. Curves of types B and C provide a more accurate description of what actually occurs, and there is little to choose between either one of them or the real data over the age range 0–20 years.

We therefore choose to work with the step function (survival type B) in most of the analysis presented in this paper; this assumption appears to offer an excellent compromise between analytic convenience and accurate description of the relevant data. Errors that may arise from this approximation are discussed at appropriate stages in later sections.

The reproductive rate of the infection

An important concept, introduced by Macdonald (1952) and refined by Dietz (1975) and others, is that of the *basic reproductive rate* of the infection, R_0 . For a directly transmitted viral infection R_0 is defined as the average number of secondary infections produced when one infectious individual is introduced into

a population where everyone is susceptible; R_0 is, in effect, Fisher's (1930) 'net reproductive value' for the infection. Thus defined, the value of R_0 depends both on biological factors having to do with the etiology of the infection, and on environmental and social factors having to do with contacts among hosts.

If the infection is endemic, some interesting relations between R_0 and epidemiological characteristics (such as the fraction of the population that are susceptible, or the average age at first infection) can be found under the assumption of 'weak homogeneous mixing', as defined above. The argument runs as follows. As the infection becomes established, the fraction of the host population who remain susceptible will decrease; the net fraction susceptible may be denoted by \bar{x} , where

$$\bar{x} \equiv \bar{X}/\bar{N}. \quad (10)$$

The total number of susceptibles, \bar{X} , and the total population, \bar{N} , are as defined earlier (see equation (1)). The assumption of weak homogeneous mixing says that the rate of appearance of new infections is linearly proportional to the number of susceptibles. Thus, on average, the number of secondary infections will be diminished below the number occurring when all individuals are susceptible, by the factor \bar{x} . That is, the value of the *effective reproductive rate*, R , is

$$R = R_0 \bar{x}. \quad (11)$$

If the infection is established at a roughly steady equilibrium value, the effective reproductive rate will be unity: at equilibrium each infection on average produces exactly one secondary infection (this commonsense result can be established with great rigour; Nold, 1979). Thus at equilibrium R_0 and the fraction susceptible, \hat{x} , are related by

$$R_0 \hat{x} = 1. \quad (12)$$

Equation (12) can be used in two ways.

On the one hand, if the equilibrium fraction of the population who are susceptible can be determined from serological or other data, equation (12) can be employed to estimate R_0 . Such estimates are discussed further in the next sub-section.

On the other hand, written in the form $\hat{x} = 1/R_0$, equation (12) can be the basis of an empirical test of the validity of the underlying assumption of weak homogeneous mixing. In deriving equation (12), we made no assumptions about how individuals acquire infection: at equilibrium before vaccination, susceptibility will be lost only by natural infection; at equilibrium after a vaccination programme is in place, susceptibility may be lost either naturally, or by immunization. Provided no other social or environmental change had taken place (no reducing of contacts by better hygiene, for instance), R_0 will remain unaltered and equation (12) produces the surprising conclusion that the fraction of the population who are susceptible to infection will remain the same after the vaccination programme as it was before (Hethcote, 1983). Fine & Clarkson (1982*b*) have used data for measles in England and Wales, before and after the advent of mass immunization, to show that the number of susceptibles has indeed remained roughly constant (at around 4–4.5 million). This is an important test of the theoretical equation (12), and more such studies are highly desirable. It must be stressed, however, that, although

equation (12) can alternatively be derived in a very elaborate way from equilibrium versions of equations (3)–(6) (see Appendix 1), it essentially rests only on the assumption of *weak* homogenous mixing, and successful tests of the relation against empirical evidence do not, in the terminology introduced above, constitute tests of the assumption of strong homogeneous mixing.

Note, however, that equation (12) cannot be satisfied if the proportion of the population who are successfully immunized, p , exceeds some critical value. As the fraction susceptible cannot exceed the fraction not successfully immunised ($\bar{x} < 1 - p$), equation (12) can only be satisfied if $R_0(1 - p)$ exceeds unity. It follows that if the proportion immunized exceeds the value

$$p > 1 - 1/R_0 \quad (13)$$

then the effective reproductive rate of the infection will necessarily be less than unity, and the infection will die out. In other words, equation (13) gives the criterion for eradication of an infection by a vaccination programme. Equation (13) incidentally indicates that infections with relatively large values of R_0 will, other things being equal, usually be more difficult to eradicate (require a higher proportion to be vaccinated) than those with small R_0 values, which is intuitively reasonable.

The above discussion assumes only weak homogeneous mixing, namely that the overall transmission rate is $\lambda\bar{X}$, with the dependence of λ on \bar{Y} unspecified. These results, and others that are discussed below, are more commonly derived in a relatively elaborate way from equilibrium versions of equations (3)–(6) in conjunction with the assumption of strong homogeneous mixing (namely that $\lambda = \beta\bar{Y}$, or, equivalently, that the overall transmission rate is $\beta\bar{Y}\bar{X}$). As indicated in Appendix 1, this less general analysis leads to an expression for R_0 that makes explicit its dependence on the various parameters: for instance, for type A survivorship ($\mu = \text{constant}$),

$$R_0 = [\beta\sigma\bar{N}]/[(\mu + \sigma)(\mu + \gamma)]. \quad (14)$$

Here the rate parameters σ and γ are characteristic of the infection itself, while the net transmission rate $\beta\bar{N}$ involves etiological, social and environmental factors. Equation (14) can be equivalently expressed as

$$R_0 = \bar{N}/\bar{N}_T, \quad (15)$$

where the ‘threshold’ population size, \bar{N}_T , is defined as

$$\bar{N}_T = (\mu + \sigma)(\mu + \gamma)/(\beta\sigma). \quad (16)$$

From equation (15) it follows that the total population density must exceed the threshold size ($\bar{N} > \bar{N}_T$) for the disease to be able to maintain itself within the population (that is, for R_0 to exceed unity). Comparing equations (10), (12) and (15) we see that at equilibrium in equations (3)–(6) the total number of susceptibles is equal to the threshold population: $\bar{X} = \bar{N}_T$. Although this threshold concept occupies an important place in epidemiology, it should be noted that equations (14)–(16) depend on the strong homogeneous mixing assumption, and are accordingly less robust than equations (11) and (12). In particular, it does not generally seem to be true that R_0 is linearly proportional to \bar{N} (see, for example, Anderson & May, 1982).

Estimating the value of R_0

A direct estimate of R_0 from expressions such as equation (14) is usually impossible, because of the difficulties inherent in obtaining estimates of the transmission parameter β .

The basic reproductive rate may, however, be estimated from equation (12) provided that the required information about the fraction susceptible is available (or can be deduced). Such an estimate has the additional advantage of being relatively robust, relying on the weak homogeneous mixing assumption.

If the force of infection, λ , is assumed to be a constant, the equilibrium number of susceptibles of age a in the absence of vaccination is

$$X(a) = N(0) \exp\left(-\lambda a - \int_0^a \mu(s) ds\right). \tag{17}$$

The corresponding number of individuals of age a is simply

$$N(a) = N(0) \exp\left(-\int_0^a \mu(s) ds\right). \tag{18}$$

These expressions are derived in Appendix 1. The total number of susceptibles, \bar{X} , now follows by integrating $X(a)$ over all ages (see equation (1)), and similarly \bar{N} is the integral of $N(a)$ over all ages. The equilibrium values of \hat{x} then follows immediately from equation (10), whence R_0 is obtained from equation (12): $R_0 = \bar{N}/\bar{X}$. In this way, it is a straightforward task to calculate R_0 in terms of λ for any specified assumption about the mortality rate $\mu(a)$.

Alternatively, these results can be expressed in terms of the age at first infection, A , which is simply the inverse of λ : $\lambda = 1/A$, equation (2.6, Appendix 2). To estimate A we require epidemiological data which records, either horizontally or longitudinally, the proportions of different age classes who have experienced the infection. This information may be obtained from age-stratified case notification records or, more accurately, from serological surveys. A worked example of the procedures employed to estimate A from case notification records is given in Appendix 2.

In particular, for a type A mortality curve ($\mu = \text{constant} = 1/L$), Dietz (1975) has derived the relation

$$R_0 = 1 + \lambda L. \tag{19}$$

Equivalently, this relates R_0 to L and A by

$$R_0 = 1 + L/A. \tag{20}$$

For the more realistic, step function, type B mortality curve, where everyone lives exactly to age L and not beyond, the corresponding expressions are

$$R_0 = \lambda L/[1 - \exp(-\lambda L)], \tag{21}$$

or, equivalently,

$$R_0 = (L/A)/[1 - \exp(-L/A)]. \tag{22}$$

For most childhood infections A is much less than L i.e. λL is large), so that an excellent approximation is

$$R_0 \simeq \lambda L = L/A. \tag{23}$$

These results are derived in Appendix 1.

As explained in the preceding sub-section, throughout most of this paper we work with the relatively realistic type *B* mortality curve. Knox (1980) also assumes this kind of mortality, but most other studies (Dietz, 1975, 1981; Hethcote, 1983) use the age-independent type *A* mortality rate.

Protection provided by maternal antibodies

Newborn infants are often immune to infections from viral agents as a consequence of the protection provided by maternal antibodies, which were passed via the placenta into the bloodstream of the unborn child during pregnancy. The duration of this protection is usually short, being of the order of 3–9 months. It is closely correlated with the half life of IgG antibodies.

The effect of this short period of immunity during infancy on the estimation of quantities such as the basic reproductive rate, R_0 , can be assessed by means of a simple modification to the basic equilibrium model described above (see Appendix 1 for details). We assume that maternally derived immunity is lost at a per capita rate, d , such that the average duration of protection, D , is $1/d$. We define a new variable $I(a)$ to denote the number of infants of age a who are protected by maternal antibodies. Other parameters, such as the force of infection λ and the mortality rate μ , remain as defined above; for simplicity (and in contrast to most of the rest of our paper) we take μ to be constant (type *A* mortality). The initial conditions become $I(0) = \mu\bar{N}$ and $X(0) = H(0) = Y(0) = Z(0) = 0$. It is here assumed that all newborn infants are immune, since for most common viral infections in unvaccinated communities the vast majority of women will have experienced the infection prior to childbirth. At equilibrium the numbers of immune infants and susceptibles of age a are then (Appendix 1)

$$I(a) = \mu\bar{N} \exp [-(\mu + d)a], \quad (24)$$

$$X(a) = \frac{d\mu\bar{N}}{(d - \lambda)} \left\{ \exp [-(\lambda + \mu)a] - \exp [-(d + \mu)a] \right\}. \quad (25)$$

The average age at infection, A , is now

$$A = [1/d + 1/\lambda]. \quad (26)$$

That is, individuals on average acquire infection at an age which is older by the amount D (i.e. $1/d$), corresponding to the period of protection by maternal antibodies. The force of the infection λ is now related to A by

$$\lambda = 1/(A - D). \quad (27)$$

The basic reproductive rate, R_0 , takes the form (for the type *A* mortality used here; see Appendix 1)

$$R_0 = \left(1 + \frac{L}{A - D}\right) \left(1 + \frac{D}{L}\right). \quad (28)$$

If D is very small in relation to life expectancy, L , as it usually is, equation (28) reduces to the form

$$R_0 \simeq 1 + \frac{L}{A - D}. \quad (29)$$

Similarly, for the more realistic type *B*, step function, mortality curve, we obtain the approximate result

$$R_0 \simeq L/(A - D). \quad (30)$$

These equations (28) and (29) for R_0 differ from the earlier equations (20) and (23), respectively, simply in that A is replaced by $A - D$. The result is intuitively reasonable, and represents a simple correction to allow for the fact that infants are not susceptible for an initial period of duration roughly D .

The important message emerging from the above analysis is that when we estimate the force of infection λ from the average age at infection A , care must be taken to allow for the period of protection by maternal antibodies. This can be done by adjusting the denominator in equation (27) to take account of the value of D .

Finally, we observe that the above theoretical analysis indeed gives results that accord with observed patterns. Fig. 2*a* shows the prediction of the simple model, equation (24), which agrees remarkably well with observed age-structured serological profiles within a community in which rubella is endemic, Fig. 2*b*.

The inter-epidemic period, T

Deterministic compartmental models of recurrent epidemic behaviour predict damped oscillations in disease incidence to a stable endemic equilibrium state. For infections such as measles and rubella this predicted damping time can be long, being of the order of many decades. Such predictions, however, differ from the patterns observed for many common viral infections where persistent, non-seasonal oscillations in disease prevalence are a notable feature. Such oscillations are often of a very regular nature, severe in magnitude, and tend to be superimposed over a shorter-term seasonal cycle. They arise as a consequence of the decay (by infection) and renewal (by births) of the supply of susceptibles within the population.

The general model defined by equations (3)–(6) yields the prediction that the weakly damped oscillations have an inter-epidemic period, T , approximately given by

$$T = 2\pi(AK)^{\frac{1}{2}}. \quad (31)$$

Here A is the average age at infection and K is the average interval between an individual acquiring infection and passing it on to a new infectee (K is estimated as the sum of the latent plus infectious periods, $K = 1/\sigma + 1/\gamma$; Anderson & May, 1982). The estimates provided by equation (31) closely mirror observed inter-epidemic periods for many common childhood infections such as measles (e.g. the 2- to 3-year cycle of measles incidence in unvaccinated communities within developed countries). This is probably because the weakly damped fluctuations predicted by the basic model can be transformed into sustained oscillations by seasonal variation in the force of infection or by the inclusion of chance elements in the growth and decay of the susceptible and infectious populations; there is a large and growing mathematical literature on this subject, which we will not pursue further here (Bartlett, 1957; Bailey, 1975; Dietz, 1976; Yorke *et al.* 1979; Hethcote, Stech & Van den Driesche, 1981; Grossman, 1980; Smith, 1983; Aron & Schwartz, 1983).

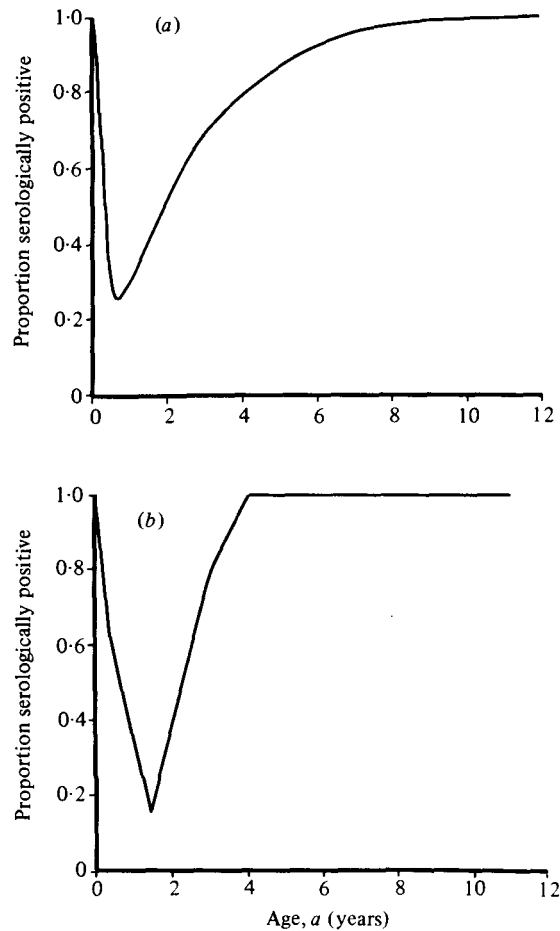


Fig. 2. Changes in the proportion of children with antibody to rubella virus with age. (a) Predictions of the simple model represented by equations (26) and (27) in the main text with parameter values $A = 2.5$ years, $D = 0.25$ years and $L = 50$ years. (b) Proportions of children in different age classes with antibody to rubella virus in two Gambian villages (data from Clarke *et al.* 1980).

We believe it to be significant that simple compartmental models can (via equation (31)) explain the essential features of many of the observed oscillatory patterns. Furthermore, such models suggest that infectious agents with high reproductive rates (large R_0 values and consequently small A values) will tend to exhibit large-scale fluctuations in incidence with short inter-epidemic periods (1-, 2- or 3-year periods), while those with low reproductive rates (low R_0 values) will exhibit low-amplitude fluctuations with long inter-epidemic periods. If the basic reproductive rate is very large and the infection induces lifelong immunity in those who recover, then the large amplitude fluctuations in disease incidence and the density of susceptibles may result in the extinction of the infection (due to chance events) during a trough in the epidemic cycle, in all but very large communities. This observation in part explains why infections such as measles will only persist endemically, without the continual introduction of infecteds, in large communities

with populations exceeding 200 000–300 000 people (Bartlett, 1957, 1960; Black, 1966; Yorke *et al.* 1979).

These aspects of the dynamics of infection, which are also highly relevant to our later exploration of the short-term dynamical consequences of vaccination programmes, are developed further in Appendix 3. Appendix 3 also provides a simple derivation of equation (31) for T .

Vaccination

In the section concerned with the basic reproductive rate, R_0 , we gave a brief discussion of the level of herd immunity required to eradicate an infection, equation (13). In this equation (13), and in much of the analyses presented below, we refer to a parameter, p , which records the proportion of a cohort of individuals (or the proportion of the total population) immunized against a specific infection. We emphasize that the parameter, p , refers to the proportion *effectively immunized*; if the efficacy of the vaccine, defined as the proportion of vaccinated individuals who develop protective immunity, is less than unity then p represents the proportion vaccinated times the efficacy of the vaccine.

In developed countries most mass vaccination programmes are directed towards children, immunizing varying proportions in a range of age classes. If susceptible children are vaccinated at an average age V , the proportion, p , of each cohort who need to be immunized in order to eradicate the infection must exceed

$$P > \frac{1 + V/L}{1 + A/L}. \quad (32)$$

Here A is the average age at infection *before* the advent of immunisation, and L is life expectancy (Anderson & May, 1982). Equation (32) can be derived exactly when vaccination is at a constant rate (namely, $1/V$) and when survival is of type A (constant μ). The expression (32) is, however, a good approximation for more general age-specific vaccination schedules and more realistic survival curves, provided the focus is on vaccination of young children (with both V and A much less than L). If vaccination is at or near birth, $V = 0$, equation (32) reduces to the earlier equation (13) (when equation (20) is used to express R_0 in terms of A). In practice, children are rarely immunized against viral infections like measles and rubella in their first year of life, because vaccination during the period when maternal antibodies are active often fails to induce protective immunity in later life.

As emphasized at the outset, vaccination has two effects within a population. The first or *direct* effect is obviously to reduce the number of individuals who are liable to experience infection. The second or *indirect* effect is that the force of infection within the community is also reduced, as a consequence of there being few infectious people; associated with this decrease in the force of infection is a decrease in the effective reproductive rate of the infection, an increase in the age at first infection, A , and a lengthening of the inter-epidemic period, T .

An estimate of the new force of infection, λ' , experienced within a population that has come to equilibrium under a specified vaccination programme, can be obtained along the lines indicated above, as encapsulated in equation (12). One first establishes the relationship between λ' and the number of susceptibles of age a , $X'(a)$, at the new equilibrium (see Appendix 1). Integrating over all ages, we

thus can calculate the overall fraction of the population who are susceptible at the new (vaccinated) equilibrium, as a function of λ' and the details of the vaccination schedule: $\hat{x}(\lambda', p)$. Estimating R_0 from the value of λ or of A in the pre-vaccinated population, we can now use the relation, $R_0\hat{x} = 1$, to calculate λ' . With λ' thus determined, we have an explicit expression for the age-specific susceptibility at equilibrium in the post-vaccination community.

The general analysis outlines in Appendix 1 can be applied to an arbitrary vaccination programme (for instance, vaccinating a proportion p of all girls at age 14 years). The expressions are relatively simple in the limit when a proportion p of each cohort is immunized at age 0: in this event, λ' is obtained from

$$(1 - p)R_0 = 1 + \lambda' L \tag{33}$$

if survival is of type A (constant $\mu = 1/L$); and from

$$(1 - p)R_0 = \lambda' L / [1 - \exp(-\lambda' L)] \tag{34}$$

if survival is of type B (everyone lives to age L). These expressions bear a simple intuitive relationship to the earlier equations (19) and (21), respectively: vaccinating a proportion p at birth effectively reduces the infection's basic reproductive rate from R_0 to $(1 - p)R_0$. Notice also that λ' is explicitly less than λ in these equations. The average age at infection, A' , at equilibrium under the new regime remains inversely related to the force of infection by $A' = 1/\lambda'$. These and more general expressions are obtained in Appendix 1.

As also stressed in the introduction, this impact of vaccination on parameters such as the average age at infection can be of major significance for infections like rubella and measles, where the risk of serious disease resulting from infection increases with age. Vaccination obviously acts for the benefit of the community as a whole by reducing the incidence of infection. But, under certain circumstances, it may also, by increasing the average age at which infections do occur, increase the total number of cases occurring in older age classes, compared with pre-vaccination levels. To assess the probability of such an occurrence, we define a ratio $\hat{w}(a_1, a_2)$ which represents the number of cases arising in the age range a_1 to a_2 at equilibrium after the vaccination programme is established, divided by the corresponding number of cases in this age range before vaccination. A vaccination programme that raises the ratio above unity is a candidate for concern. For the general model defined earlier, at equilibrium new infections in the age class a appear at the rate $\lambda' X(a, \lambda')$, so that $\hat{w}(a_1, a_2)$ is

$$\hat{w}(a_1, a_2) = \int_{a_1}^{a_2} \lambda' X(a, \lambda') da / \int_{a_1}^{a_2} \lambda X(a, \lambda) da. \tag{35}$$

From equation (35), in combination with the earlier result for λ' , $\hat{w}(a_1, a_2)$ can be calculated for any specific set of assumptions about the vaccination programme. Such results are presented in Appendix 1. We cite only one in the main text, because it helps illustrate the general trends. If a proportion p of each cohort are vaccinated at birth, and type B survival is assumed, \hat{w} takes the form

$$\hat{w}(a_1, a_2) = (1 - p) \frac{[\exp(-\lambda' a_1) - \exp(-\lambda' a_2)]}{[\exp(-\lambda a_1) - \exp(-\lambda a_2)]}. \tag{36}$$

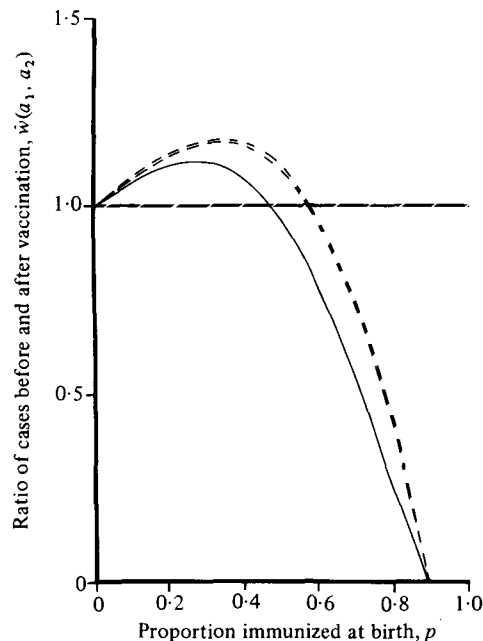


Fig. 3. The ratio $\hat{w}(a_1, a_2)$ of cases after vaccination of a proportion, p , of children at birth divided by those before vaccination in the age range $a_1 = 16$ years to $a_2 = 40$ years. —, Prediction of equation (35) in the main text in which survival is assumed to be type *A*. ---, Predictions of equations (35) in which survival is assumed to be either type *B* or type *C*. The predictions are virtually identical.

Here λ' is given explicitly by equation (34). The factor $(1-p)$ comes from the direct herd effects of vaccination, and acts to reduce \hat{w} as p increases. But as p increases, indirect effects act to decrease λ' , and the factor inside square brackets in the numerator becomes larger than the corresponding factor in the denominator. Whether the net outcome of these countervailing effects causes \hat{w} to increase or to decrease as p increases depends on the specific values of a_1 , a_2 and R_0 .

The predictions of equation (36), and of the corresponding expressions obtained by assuming survival is of type *A* or type *C* form (see Fig. 1), are illustrated in Fig. 3. Here a proportion p are vaccinated at birth, and we plot $\hat{w}(16, 40)$ for the age range 16–40 years, under the assumption that A is 8 years and L is 75 years; this roughly corresponds to the circumstances of interest for rubella. Several interesting points emerge from Fig. 3. First, as observed by Knox (1980) and Dietz (1981), in this situation the equilibrium ratio \hat{w} rises above unity for low to moderate levels of vaccination coverage, p . Secondly, the calculations based on the age-independent mortality curve of type *A* (as used by Dietz, 1981 and Hethcote, 1982) give significantly different results from those obtained by using type *B* (as used by Knox, 1980) or the quite accurate type *C* survival curves. Thirdly, the results for type *B* and type *C* mortality are effectively indistinguishable, even though the type *C* curve gives a significantly better fit to the mortality data themselves (see Fig. 1); this concordance provides some justification for our decision to use the mathematically simpler type *B* survival in most of the subsequent calculations.

Age and the risk of serious disease

The discussion in the preceding section was motivated by the fact that the risk of serious disease resulting from certain viral infections increases with age. As mentioned in the introduction, and fully documented below, measles provides one example: the risk of measles encephalitis, with common sequelae of permanent brain damage, appears to rise approximately linearly with age in the range 1–20 years (at least in the U.S.A. around 1973–5). Likewise, the fact that rubella represents a serious risk mainly to the offspring of women who contract it early in pregnancy was mentioned in the introduction, and is documented in detail below.

To assess the impact of vaccination on the incidence of measles encephalitis or of CRS, it is necessary to define a risk function whose value varies with age in accord with the observed risk to patients or mothers who contract the infection at various ages. We define this *risk function* as $m(a)$. For measles, it denotes the probability that a case of measles at age a results in a case of measles encephalitis. For rubella, the risk function is linearly proportional to the probability that a woman is pregnant at age a , and we may therefore (in calculating ratios) take $m(a)$ to be the age-specific fertility.

The ratio $\hat{\rho}(a_1, a_2)$ is defined as the number of cases developing serious disease in the age range a_1 to a_2 , at equilibrium after the vaccination programme is established, divided by the corresponding number of serious cases before vaccination. This ratio differs from \hat{w} , which measures only the ratio of the incidence of infection itself, by the incorporation of the risk function $m(a)$:

$$\hat{\rho}(a_1, a_2) = \int_{a_1}^{a_2} m(a) \lambda' X'(a, \lambda') da \bigg/ \int_{a_1}^{a_2} m(a) \lambda X(a, \lambda) da. \quad (37)$$

In general, we are likely to be interested in the ratio of the total number of serious cases, before *versus* after vaccination; this ratio is essentially $\hat{\rho}(0, \infty)$. Clearly, all such calculations followed the lines laid down in the preceding section, with the additional complication of the risk function $m(a)$.

The above discussion pertains entirely to the *statics* of infection, comparing different equilibrium states. We strongly emphasize that all this analysis rests on the assumption of weak homogeneous mixing, and does not involve the more restrictive assumption of strong homogeneous mixing.

Dynamical behaviour following vaccination

So far, we have dealt almost exclusively with comparisons among different steady-state situations. We now move on to analyse the time-dependent changes that arise when a vaccination programme, or other perturbation to the original steady state, is implemented.

Such studies of short-term dynamical effects of vaccination programmes are an important supplement to the more usual studies of the eventual steady state, for two main reasons.

First, when a programme of immunizing a proportion of each yearly cohort of children is initiated, it will often take 20 years or more before most of the children and adolescents have been given the option of vaccination. In practice, therefore,

the degree of artificially induced herd immunity within the total population will tend to change gradually over a period of many years, with the force of infection declining continually over this time. The total density of susceptibles will remain approximately constant over this period, but the proportion immune will change in character from immunity largely being acquired via infection to a state in which immunity is predominantly the result of immunization.

Secondly, as indicated earlier, many viral infections of childhood exhibit regular, non-seasonal fluctuations in incidence. Sudden perturbations to such oscillatory systems, such as induced by extensive immunization, may induce complex epidemiological changes which are difficult to predict on purely intuitive grounds. For example, immunization may initially induce a marked reduction in disease incidence, but on a longer time span the community may experience periods of high incidence alternating with periods of low incidence, with periods of many years between peaks.

Our studies of the dynamical behaviour are based on the partial differential equations (3)–(6). The mathematical details are presented in Appendix 4; in what follows we very briefly sketch the nature of the biological assumptions that are made. As mentioned in conjunction with the general equations (3)–(6), in this paper we restrict attention to developed countries, in which the net birth and death rates are almost exactly in balance (i.e. we assume a total population, \bar{N} , of constant size) and in which little mortality is associated with viral infections like measles and rubella (i.e. $\alpha = 0$). In all our studies of short-term dynamics we also assume type *B* survival (as justified in the discussion surrounding Fig. 3). Before the introduction of some specific vaccination programme at time $t = 0$, we assume that the system is at equilibrium and that the force of infection, λ , is independent of age. These and other assumptions are discussed later, in the section on ‘Future Research’.

The system of equations (3)–(6) does not by itself give a complete description of the time- and age-dependent changes provided by initiating a vaccination programme: we must also specify an explicit relation between the subsequent time-dependent force of infection, $\lambda(t)$, and the total number of infectious individuals, $\bar{Y}(t)$, or some equivalent epidemiological variable. To this end, we make the previously discussed assumption of strong homogeneous mixing (which is almost invariable in such studies), namely that $\lambda(t) = \beta \bar{Y}(t)$ where the transmission parameter β is a constant (see equation (7)).

The system of equations (3)–(6), supplemented by a term describing the transfer of individuals from the susceptible class to the immune class by vaccination, and with $\lambda(t)$ related to $\bar{Y}(t)$ by equation (7), can be solved numerically. As is so often the case with sets of coupled partial differential equations, the numerical methods must be chosen with care; several different time scales are important in equations (3)–(6), and numerical approximation of the continuous derivatives by an inappropriately coarse finite time step, for example, can generate spurious results. As indicated in Appendix 4, we can in fact do a bit better than crude numerical integration of equations (3)–(6). An explicit expression for the age-specific number of susceptibles, $X(a, t)$, can first be obtained in terms of $\lambda(t)$, and then a set of ordinary differential equations for $\bar{X}(t)$, $\bar{H}(t)$ and $\lambda(t)$ (or, equivalently, $\bar{Y}(t)$) can be integrated numerically, to give an efficient scheme for computing $\lambda(t)$, $X(a, t)$

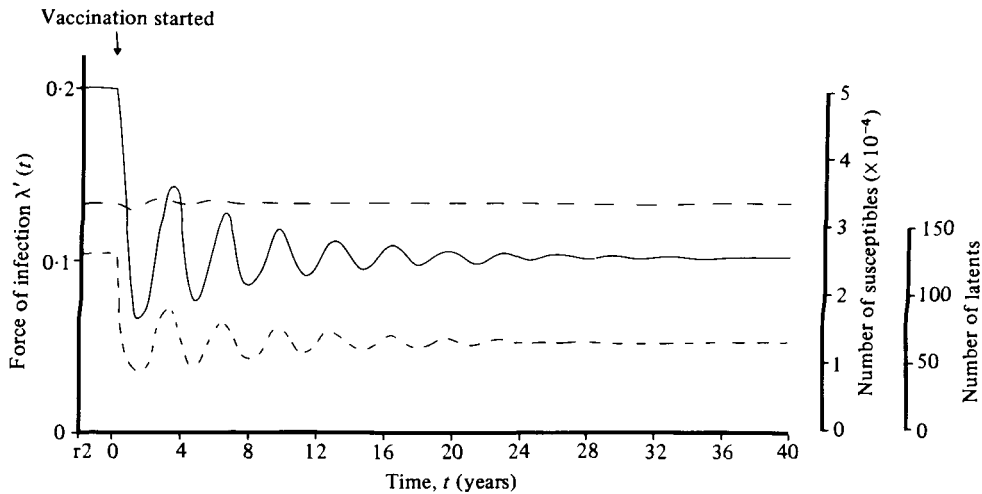


Fig. 4. Numerical solutions of equations (44)–(46) in the main text with parameter values $p = 0.6$, $\lambda = 0.2 \text{ yr}^{-1}$, $\bar{N} = 500000$, $\sigma = \gamma = 52.14 \text{ yr}^{-1}$, $R_0 = 15$, $L = 75$ (survival type *B*). Vaccination is initiated at time $t = 0$, and 60% of 2-year-old children are vaccinated each year. The three trajectories denote changes in the density of susceptibles (---) and latents (---) plus changes in the force of infection $\lambda'(t)$ (—).

and thence the time-dependent ratios $w(a_1, a_2; t)$ or $\rho(a_1, a_2; t)$. A typical set of results are illustrated in Fig. 4; this and a series of other such theoretical results are discussed later in the light of available data for vaccination programmes against measles and rubella in the U.K. and the U.S.A.

Most previous studies have focused on comparing the final equilibrium state after mass immunization with the initial, pre-immunization equilibrium. Two significant exceptions are the recent studies of rubella by Knox (1980) and of measles by Cvjetanovic *et al.* (1982), both of which present computer studies of the impact of immunization on the population dynamics of infection. We believe that both these studies offer important and new insights, but that some of their conclusions may be in error (as a result of faults in the mathematics).

Knox's study of the dynamics of the incidence of rubella following the introduction of mass vaccination employs a set of difference equations, which describe changes in the number of cases of CRS under different regimes. In particular, Knox uses the apparently harmless approximation of changing the magnitude of the force of infection in one-year time steps (the changes depend on the total number of infections in the previous year). But many of the essential dynamical processes in this system are, in fact, keyed to the time scale, T , described by equation (31); the inter-epidemic period is one natural time scale for the system described by equations (3)–(6). Up-dating λ once a year corresponds, in effect, to assuming that $K = 1$ year in equation (31) when actually for rubella $K \simeq 2\text{--}3$ weeks (K is the average time between acquisition and transmission of infection, roughly equal to the average duration of latent plus infectious periods). Because the natural time scale T depends on $K^{\frac{1}{2}}$, Knox's procedure, which does not at first glance seem unreasonable, has the effect that the epidemiological changes generated by his computer models all take place on time scales that are about 4–5 times too long.

If his simulation of rubella vaccination programmes is repeated with λ updated every 3 months, we obtain essentially the same graphical results except that the time axes are halved; if λ is updated every 4 years, the time axes are doubled. The explicit mathematics underlying these assertions is given in Appendix 3. All this can be read as a cautionary tale: the time steps used in approximating the partial differential equations (3)–(6) need to be chosen carefully.

Cvjetanovic *et al.* (1982) also employed a set of difference equations to examine the impact of various levels of vaccination coverage on the dynamics of measles within large populations. Making extensive use of public health data for measles in Britain, Germany and elsewhere, they concluded that immunization of 60–70% of successive cohorts of infants could eventually (in 10–20 years) eradicate measles. This is a surprising conclusion, being much lower than other estimates that use essentially the same data to determine the age at infection, A , and other such parameters (Anderson & May, 1982, and references therein). Cvjetanovic *et al.* use an appropriate time step (updating all relevant variables every 10 days), but they do not describe how the force of infection is modified in response to changes in the number of infectious individuals and other such factors. It appears to us that they hold λ fixed, at age-specific values deduced from data from a community in which a roughly 60% immunization level had been sustained. Under this assumption of unvarying λ , any increase in the proportion immunized, no matter how small, will lead to eventual eradication; as the initial equilibrium, the effective reproductive rate is unity, $R = 1$, and now vaccination removes susceptibles without any compensating decrease in λ being allowed, whence R must fall below unity and the infection dies out. The work of Cvjetanovic *et al.* is exemplary in the way the model is solidly based on data. Assessment of the dynamical consequences of a vaccination programme, however, needs more than existing data; it also needs some concrete assumption about the way the force of infection will change in response to other epidemiological changes.

We conclude this section by again stressing that our predictions about disease *dynamics* involve the assumption of strong homogeneous mixing, which we regard as less justifiable than the assumption of weak homogeneous mixing, which underpins our studies of disease *statics*.

RUBELLA: EMPIRICAL BACKGROUND

Many mathematical studies of disease dynamics are open to the criticism that they give insufficient attention to estimating the parameters of the model from observed data. Thus, in a recent review, Becker (1979) notes that of 75 papers on epidemiological models published since 1974, only 5 contain references to, or treatment of, empirical data. A case in point is the numerical simulations of the impact of various vaccination programmes on the epidemiology of rubella by Knox (1980) and, following him, by Dietz (1981): although seminal, these studies all rest on an estimate of λ , the force of infection, that derives from the single qualitative observation that approximately 70% of 14-year-olds are immune.

In this section we therefore present a summary of quantitative data that are available on the epidemiology of rubella. These data provide the basis for our analyses of the impact of vaccination, described in the following section.

Table 1. *Latent ($1/\sigma$) and infectious ($1/\gamma$) periods for rubella and measles*

Infection	Latent period (days)	Infectious period (days)
Measles	6-9	6-7
Rubella	7-14	11-12

Symptoms of rubella infection are few in children, and as many as 20-50% of cases may occur without an evident rash. It is the hazard of significant congenital defects in offspring of women who acquire rubella during pregnancy that motivates efforts to control the disease by immunization; this association between congenital abnormalities and maternal rubella during pregnancy was first made in Australia in 1941 (Gregg, 1941). Congenital rubella syndrome (CRS) occurs among 20-50% of infants born to women who had acquired inapparent or apparent rubella infection during the first trimester of pregnancy, with decreasing frequency thereafter (Benenson, 1975). The syndrome includes cataracts, microphthalmia, mental retardation, deafness and cardiac defects. The nature, incidence and pathogenesis of these abnormalities have been reviewed by Hanshaw & Dudgeon (1978).

Rubella is worldwide in distribution except in remote and isolated communities. Transmission is direct, by droplet spread or direct contact, and virus may be recoverable from the nasopharyngeal secretions, blood, urine and faeces of infected persons. The incubation period (time from infection to appearance of symptoms) is from 14 to 21 days, while the infectious period is about 1 week before and at least 4 days after the onset of rash. Typical ranges for the latent and infectious periods are given in Table 1.

The average age at infection, A

The epidemiology of rubella, as typified by cross-sectional serological surveys, stratified by age, or by case notification records, varies among different localities and communities depending on factors such as community size, net birth rate and social and environmental conditions. In illustration of this, Fig. 5 records nine examples of the prevalence of those who have experienced rubella infection in various age classes of different communities throughout the world. As documented in Table 2, the average age at infection, A , varies from 2-3 years in Gambia during 1976 to between 13 and 16 years in the U.S.A. during 1978-80. CRS was not a cause for concern in the Gambian community since virtually 100% of people above the age of 5 had experienced rubella infection (Clarke *et al.* 1980). In contrast, in Great Britain prior to the introduction of immunization against rubella in 1970, roughly 10-15% of women of age 20 years were susceptible to infection (Urquhart, 1980; Clarke *et al.* 1979).

The inter-epidemic period, T

The incidence of rubella in Europe and North America, before wide-spread immunization, fluctuated both on a seasonal and a longer-term time scale. The long-term time scale was characteristically of variable period, ranging from 2 to 9 years in the U.S.A. and Great Britain. The average inter-epidemic period was of the order of 4-5 years. With latent and infectious periods of roughly 12 days

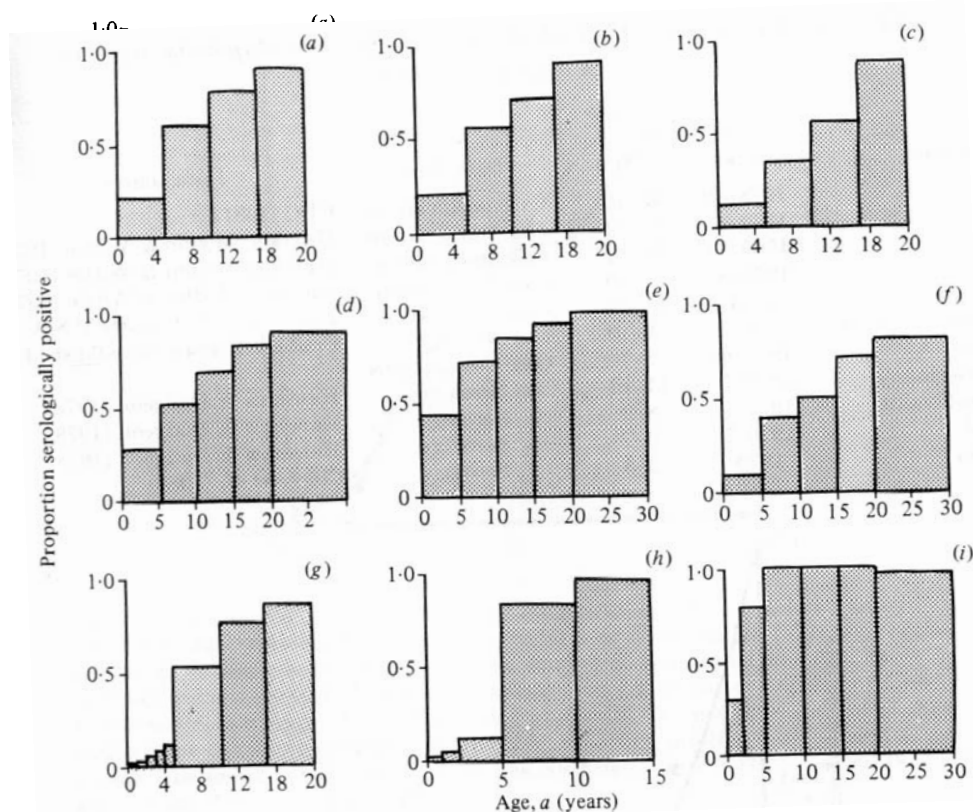


Fig. 5. Age-prevalence curves (based on horizontal studies) of the proportions of different age classes who have experienced an attack of rubella. (a)–(c), Data from Illinois, Massachusetts and New York City, U.S.A. for three different periods: (a) 1966–8; (b) 1969–71 and (c) 1972–4. Immunization was initiated in 1969 (Hayden, Modlin & Wittle, 1977; based on case notification records). (d), Data from West Germany 1970–7 (Hanshaw & Dudgeon, 1978; based on serology). (e), Data from Poland 1970–7 (Hanshaw & Dudgeon, 1978; based on serology). Graph (f), data from the United Kingdom 1970–7 (Hanshaw & Dudgeon, 1978; based on serology). (g), Data from Baltimore 1943 (Public Health Reports, U.S.A.; based on case notifications). (h), Data from Scotland (based on case notifications). (i), Data from Gambia 1966–76 (Clarke *et al.* 1980; based on serology). In all graphs, immunity resulting from maternal antibodies is not recorded.

each (Table 1) and an average age at infection A of between 8 and 10 years (Table 2) the basic model (see equation (31)) predicts an inter-epidemic period of approximately 4–5 years, a figure in agreement with that observed. In Baltimore, during the period 1931–64, for example, the average period between major peaks in rubella incidence was approximately 5 years. Within the Gambian community, where the average age at infection was between 2 and 3 years of age, theory predicts an inter-epidemic period of roughly 2–3 years in length. Empirical evidence suggests, however, that the observed period is much longer, perhaps as a consequence of the small sizes of the communities studied (population sizes 400–800, Clarke *et al.* 1980).

Table 2. Average age, A , at which rubella infection is typically acquired in different countries

Location	Time period	Average age, A (years)	Data base	Data source
U.S.A.	1978-80	13-16	Case notifications	CDC (1981 <i>a</i>)
U.S.A.	1972-4	12-14	Case notifications	Haydon, Modlin & Wittle (1977)
U.S.A.	1969-71	10-11	Case notifications	Haydon, Modlin & Wittle (1977)
U.S.A.	1966-8	9-10	Case notifications	Haydon, Modlin & Wittle (1977)
U.S.A.	1943	10-11	Case notifications	Public Health Reports U.S.A.
England and Wales	1977	9-10	Serology	Craddock-Watson (unpublished data)
Scotland	1950-60	6-7	Case notifications	
West Germany	1970-7	11-12	Serology	Hanshaw & Dudgeon (1978)
Czechoslovakia	1970-7	8-9	Serology	Hanshaw & Dudgeon (1978)
Poland	1970-7	6-7	Serology	Hanshaw & Dudgeon (1978)
Gambia	1976	2-3	Serology	Clarke <i>et al.</i> (1980)

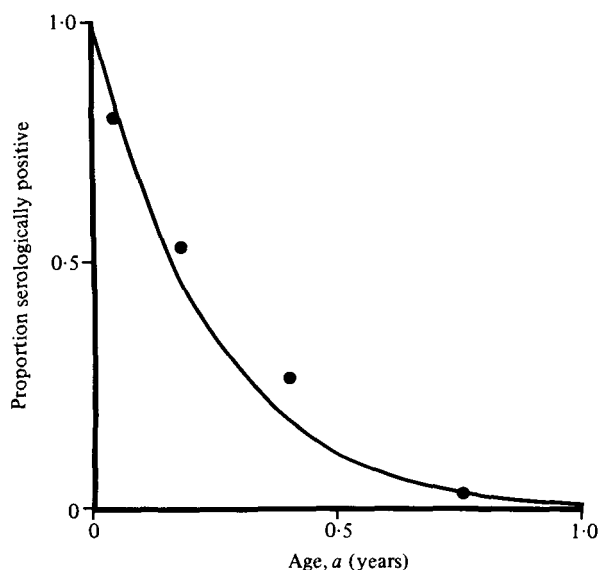


Fig. 6. The prevalence of rubella IgG antibody in different age groups of infants from the Manchester area of England in 1977. Sera from infants were obtained from candidates for adoption (unpublished data from J. Craddock-Watson). ●, Observed values; —, best-fit exponential decay model, with an expected duration of stay in the positive class of approximately 0.25 years. The total number of sera tested was 236.

Maternal antibodies

Protection provided by maternal antibodies appears to last for a maximum period of one year. The decay in serologically positive individuals in the first year of life in communities in which rubella is endemic, however, is rapid and the average period during which infants have detectable antibody levels is roughly 3 months. This trend is illustrated in Fig. 6, which is based on a serological survey by Craddock-Watson (unpublished data) in 1976-7 of a local community in Manchester, England. Roughly 80% of newborn infants had positive sera. Similar

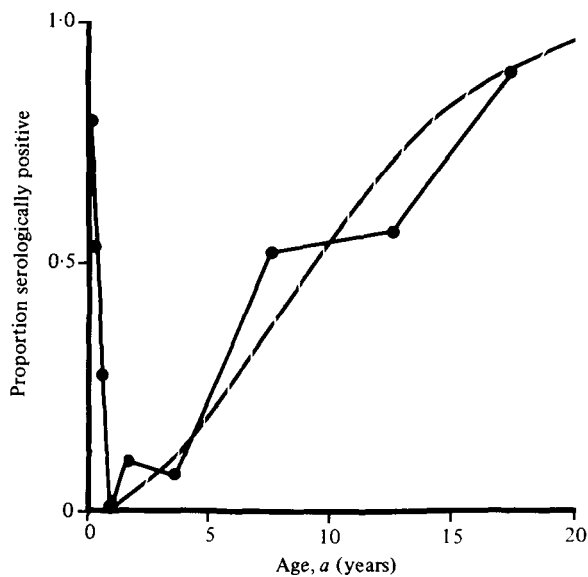


Fig. 7. Similar to Fig. 6 but recording the prevalence of infants, children and young adults with IgG antibody to rubella (Manchester area of England in 1977; unpublished data from J. Cradock-Watson). The total number of sera tested was 537. ●, —, observed values; ---, fit of an age-prevalence model with an age-dependent force of infection $\lambda(a)$ (see Appendix 2). The fitting procedure does not take account of those positive due to maternal antibodies, and the proportion positive is set at zero at age 1 year. The linear model $\lambda(a) = m + va$ has coefficients $m = 0.0321$, $v = 0.0118$. The average age A at infection is 9.23 years.

rates of decay were observed in the Gambian community studied by Clarke *et al.* (1980), even though 100% of newborn infants had positive sera.

The force of infection

As indicated by the data recorded in Table 2, the average force of infection varies greatly in different localities throughout the world. A number of studies indicate that the rate is age-dependent, tending to rise to a plateau during childhood. In Cradock-Watson's study of a community in England, for example, the rate of infection rises approximately linearly between the ages of 1 and 20 years. Fig. 7 displays the serological data obtained in this study and records the fit of an age-dependent infection model (see Appendix 2) in which the force of infection is a linear function of age. In this community the average age at infection, A , was approximately $9\frac{1}{4}$ years. This value seems to be typical of unvaccinated communities in developed countries (Table 2). The average value of the force of infection, λ , over all age classes is simply the inverse of the average age at infection corrected for the average length of protection provided by maternal antibodies (see equation (26)). In our analyses of the impact of vaccination on the incidence of CRS in Britain and North America we assume that, prior to immunization, the average age at infection was between 9 and 10 years of age. Note that this value, which is based on the available data, is somewhat less than the values assumed by Knox (1980), Dietz (1981) and Hethcote (1983) in their studies of this problem.

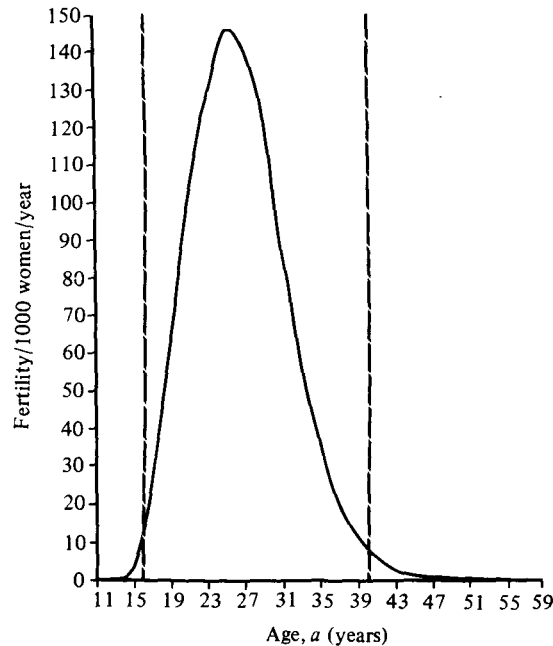


Fig. 8. The age-specific fertility of women, $m(a)$, in England and Wales in 1980. The fertility rate is defined per 1000 women per year. A precise empirical fit to the data in the age range 16–40 years of age (encompasses 99% of all recorded births) is obtained by the polynomial $m(a) = c_1 + c_2 a + c_3 a^2 + c_4 a^3 + c_5 a^4 + c_6 a^5 + c_7 a^6$ with coefficients $c_1 = 5256.0$, $c_2 = -1058.0$, $c_3 = 78.47$, $c_4 = -2.59$, $c_5 = 0.0342$, $c_6 = 0.0$, $c_7 = -0.2523 \times 10^{-5}$ ($r^2 = 0.997$). The data are from the Registrar General's Statistical Review for 1980.

Congenital rubella syndrome and fertility rates

The annual number of cases of CRS in infants born to mothers in various age classes will obviously depend, among other things, on age-specific fertility rates. For most developed countries today, the pattern of age-specific fertility is similar to that recorded in Fig. 8 for England and Wales in 1980. Peak fertility occurs at around 25 years while 99% of all births occur in the age range 16–40 years of age. The number of unborn infants at risk in a given year will therefore be proportional to the sum over the age range 16–40 years of the age-specific fertility rate times the age-specific incidence of rubella infection. We therefore define the risk function, $m(a)$, for the incidence of CRS to be the age-specific fertility rate.

Vaccination policies in the U.S.A. and the U.K.

The stated purpose of immunization against rubella is to prevent infection in pregnant women and subsequent CRS. There is a disagreement, however, about the best vaccination policy to achieve this end (Knox, 1980).

In the U.S.A. rubella control programmes in the early stages after the licensing of the vaccine in 1969 emphasized vaccination of pre-school and elementary school children (both boys and girls). This strategy resulted in a dramatic decline in reported rubella and virtually eliminated the characteristic long-term cycle of

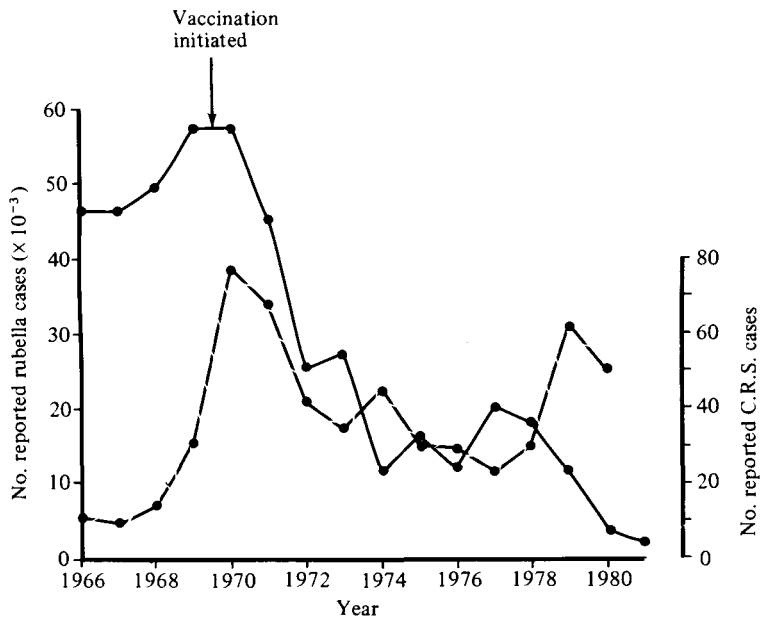


Fig. 9. Reported cases of rubella (—) and congenital rubella syndrome (---) in the United States between 1966 and 1981 (data from Centers for Disease Control, U.S. Department of Health and Human Services).

epidemic rubella (CDC, 1981*a*). Concomitant with this trend, there was a marked change in the age characteristics of reported rubella cases. This feature is illustrated in Fig. 5 by graphs *a*, *b*, and *c*; these record the change in the proportion of cases occurring in different age classes in Illinois, Massachusetts and New York City over the period 1969–74 (Hayden, Modlin & Wittle, 1977). The average age at infection, *A*, over this period changed as result of immunization from 9–10 years of age to 13–14 years (see Table 2). In the U.S.A. as a whole the average age had risen to roughly 16 years of age by 1980. In 1979, for example, approximately 70% of reported rubella causes were among individuals above 15 years of age (CDC, 1981*a*). The number of reported rubella cases has continued to decline, such that between 1978 and 1980 the percentage change was 78.6% (Fig. 9). Much of the recent decline is due to the Childhood Immunization Initiative which began in 1977, whose goal was to achieve and maintain immunization levels in excess of 90% for all childhood vaccine-preventable diseases. The measles elimination initiative, begun in 1978, has further influenced reduction in the incidence of rubella since most of the measles vaccine administered has been given as MMR (measles, mumps, rubella vaccine) or MR (measles, rubella vaccine). The current strategy for rubella control in the U.S.A. is based on continued routine vaccination of all children 15 months of age or over, vaccination of all schoolchildren not vaccinated in infancy, and vaccination of susceptible adults (particularly females and/or hospital personnel). Increased efforts to vaccinate adolescents and young adults were prompted by continued reporting of between 20 and 70 cases of CRS per year from 1971 to 1979 (CDC, 1981*a*). This trend is illustrated in Fig. 9. Also of interest in this figure is the relative impact of vaccination on the incidence of

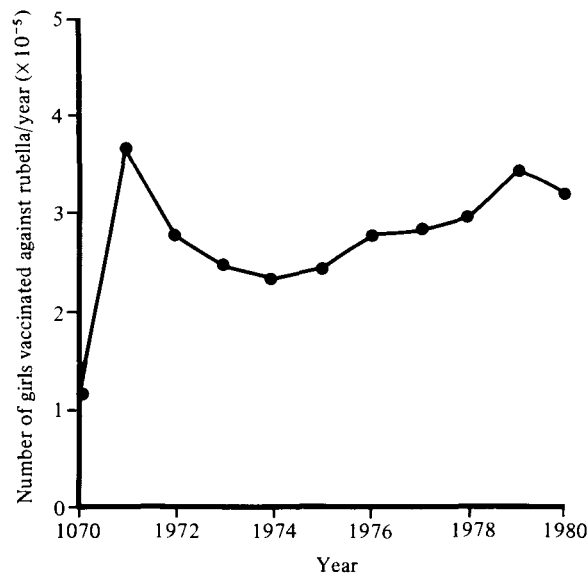


Fig. 10. The number of girls between the ages of 10 and 15 years vaccinated against rubella in England each year between 1970 and 1980 (data from the Department of Health and Social Security, Statistics and Research Division, U.K.).



Fig. 11. The proportion p of girls in England who were immunized against rubella infection by the end of 1980 in the age range 10–15 years (data from the Department of Health and Social Security, U.K.).

rubella and on the number of reported CRS cases. The U.S.A. immunization policy has had a marked impact on incidence, but much less influence on CRS. Also note the hint of a 4- to 5-year cycle in reported CRS cases during the period 1968–80. It is thought that the current strategy may eventually eliminate both rubella and CRS in the U.S.A. once the overall level of herd immunity exceeds 90%.

The adopted policy in the U.K., which differs from that in the U.S.A., is to

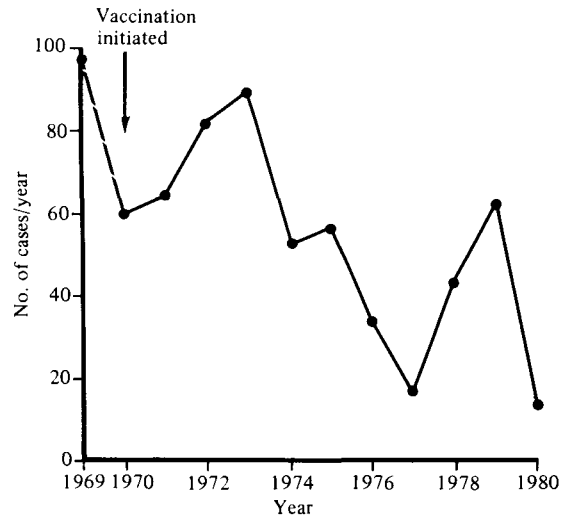


Fig. 12. The annual number of reported cases of congenital rubella syndrome in the years 1970–80 in England, Scotland and Wales. For a given year the total number of cases is based on diagnoses up to 4 years after the birth of the child (the figures for 1979 and 1980 are therefore only provisional values). The figure for 1969 is a rough estimate based on reported cases in the previous 4 years (data from Dr W. C. Marshall, The Hospital for Sick Children, Great Ormond Street, London).

vaccinate girls, and girls only, at 10–15 years of age. This is then supplemented by selective post-partum vaccination in women found not to have antibodies to rubella during antenatal care. More recently, vaccination has been recommended to all seronegative women of childbearing age. Vaccination of schoolgirls was initiated in 1970, and from 1971 to 1980 between 200 000 and 375 000 individuals were immunized annually (Fig. 10). The average age at vaccination, V , had been approximately 12 years of age, and by the end of 1980 roughly 80% of 13-year-old girls had been immunized (Fig. 11). This policy had led to a decline in the proportion of seronegative women attending antenatal clinics. In Glasgow the proportion fell from 14.2% in 1976 to 10.2% in 1979 (Urquhart, 1980); in Ayrshire from 29.6% in 1974 to 11.1% in 1978 (McCartney & Ross, 1979); and in England in 20- to 22-year-old women from 11.5% in 1976 to 4.4% in 1979 (Clarke *et al.* 1979; Grist, Reid & Young, 1981). A considerable degree of variation in these trends is apparent in different regions of the U.K. due to factors such as the non-availability of susceptibility tests (Edmond *et al.* 1980) and variation in the efficiency of postnatal administration of vaccine. A national register of CRS cases in England and Wales was started only in 1971; it is therefore not possible to examine the overall impact of the U.K. vaccination policy on the incidence of this disease by looking at trends before and after the initiation of the control programme.

The numbers of reported CRS cases in England and Wales over the past 10 years are recorded in Fig. 12. The overall trend is for a decrease in CRS; note, however, the suggestion in these data of a 4- to 6-year cycle in peak incidence. Since rubella is not a notifiable infection in the U.K., the impact of immunization on the overall incidence of rubella cases is not known. Some caution is necessary in the

interpretation of the data presented in Fig. 12, because the efficiency of diagnostic procedures has improved over the period 1971–81. It is believed that one consequence of this is an improved rate of detection of infection during pregnancy, leading to an increase in the number of terminations due to rubella. The downward trend displayed in Fig. 12 may therefore be an artifact arising from improvements in pre-natal screening.

RUBELLA: ANALYSIS AND MODEL PREDICTIONS

This section is divided into two parts. The first considers the steady-state or equilibrium condition towards which a population may converge, in the long term, under the influence of a particular vaccination programme. The second part considers the short-term dynamics of the infection within the population, as it begins the passage to a new steady state following the initiation of control measures.

Equilibrium or steady-state properties

Our assessment of the impact of different vaccination schedules on equilibrium properties is based on the ratio $\hat{\rho}(a_1, a_2)$. This ratio (defined in a given year at equilibrium) is the number of women in the age range 16–40 ($a_1 = 16, a_2 = 40$) who acquire infection with rubella during pregnancy when a defined vaccination programme is adopted, divided by the number of women in the same age range who acquire rubella infection during pregnancy prior to the instigation of immunization. We focus on a comparison of the vaccination policies in the U.K. and U.S.A.; these we define, respectively, as vaccination of a proportion p of girls at age 12 years and vaccination of a proportion p of boys and girls at age 1 year. We consider a community within a developed country, assuming that survival is the step function form (survival type B , see Fig. 1) and that the age-specific fertility rates are as depicted in Fig. 8. We also assume, in the absence of clear evidence to the contrary, that successful immunization induces permanent immunity to infection (Preblud, Serdula & Frank, 1980). The model employed to calculate the ratio $\hat{\rho}(a_1, a_2)$ is as defined in Appendix 1.

The average age at infection, A , in the community prior to vaccination (which, remember, is an inverse measure of the value of the basic reproductive rate, R_0) may have either a considerable or a negligible impact on the ratio $\hat{\rho}(a_1, a_2)$, depending on the vaccination policy adopted. As shown in Fig. 13, under the U.S.A. vaccination policy the ratio rises above unity when the average age at infection, A , prior to control is less than 12 years of age. The degree to which $\hat{\rho}$ exceeds unity, and for what range of values of p (the proportion vaccinated), depends on the precise value of A . Conversely, under the U.K. policy (where girls are vaccinated at 12 years of age), the value of A has a negligible impact on the ratio for all values of p .

The U.K. policy is consistently better at reducing the number of women of childbearing age at risk of infection, for all but very high levels of immunization coverage, p . The principle behind this prediction is that the U.K. policy has much less impact on the average force of infection than does the U.S.A. policy, and hence allows girls to acquire immunity by natural infection before reaching the

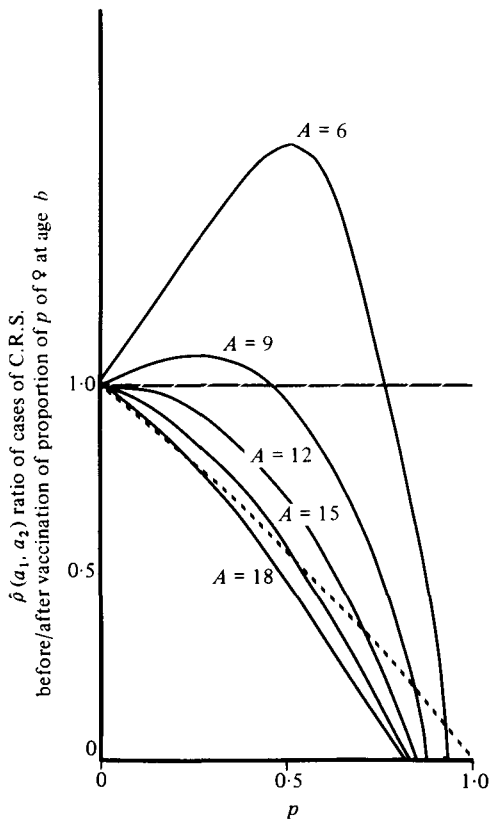


Fig. 13

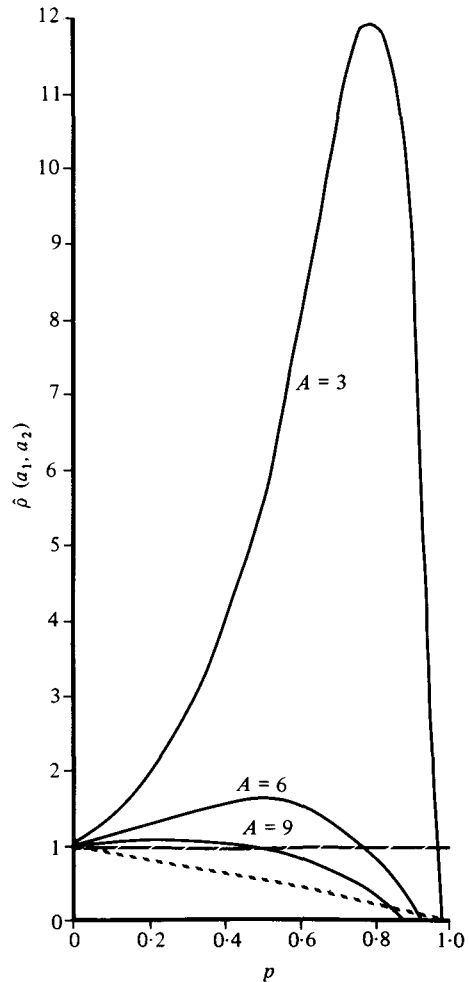


Fig. 14

Fig. 13. Rubella. The equilibrium ratio $\hat{\rho}(a_1, a_2)$ of rubella cases in pregnant women in the age range 16–40 years after vaccination of a proportion p at age b divided by the cases before vaccination (see Appendix 4). The age-specific fertility function $m(a)$ employed to calculate $\hat{\rho}(a_1, a_2)$ is as defined in Fig. 8, and we assume a type B survival function with a life expectancy of 75 years. —, Changes in the ratio for various values of p under the U.S. policy where boys and girls are vaccinated at age 1 year ($b = 1.0$) for various values of the average age at infection, A , prior to vaccination ranging from 6 to 18 years. The dashed line intersecting the horizontal axis at $p = 1.0$ is the ratio for the U.K. policy where girls and only girls are vaccinated at age 12 years ($b = 12$). For A values between 6 and 18, the value of the ratio $\hat{\rho}(a_1, a_2)$ is virtually identical for the U.K. policy for all values of p . The horizontal dashed line denotes the ratio value of unity.

Fig. 14. Rubella. Identical to Fig. 13 but including changes in $\hat{\rho}(a_1, a_2)$ for an average age at infection, A , of 3 years (to mirror events in the Gambian community discussed in the main text), ---, See legend to Fig. 13.

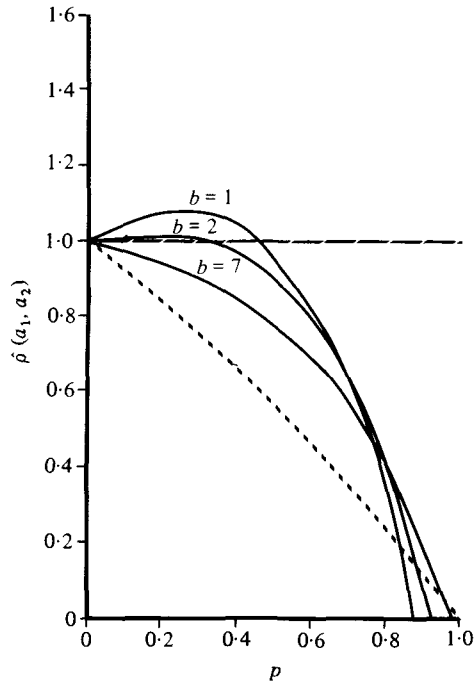


Fig. 15. Rubella. Identical to Fig. 13 but with the value of A fixed at 9 years of age. —, Changes in the ratio $\hat{\rho}(a_1, a_2)$ with p for the U.S. vaccination policy where boys and girls are vaccinated at age $b = 1$ year, $b = 2$ years and $b = 7$ years. The horizontal and dashed lines are as defined in the legend to Fig. 13.

childbearing age range (16–40 years). An extreme example of the predicted impact of the U.S.A. policy is displayed in Fig. 14, where the ratio $\hat{\rho}(a_1, a_2)$ is plotted for a community in which the average age at infection before control was set at 3 years (as in the Gambian community discussed earlier; see Table 2); the ratio only falls below unity when the level of immunization exceeds 96%. In such extreme situations, vaccination is of benefit to the individual but can act to the considerable disadvantage of the community as a whole.

In developed countries such as the U.K. and the U.S.A., where the value of A prior to control was approximately 9 years of age, the U.S.A. policy is only of greater benefit than the U.K. policy when immunization levels exceed 84%. Some support for this estimate is provided by the observed trends in CRS cases after immunization in the U.S.A. and the U.K. (Figs. 9 and 12). In the U.K., there has been an overall decline in the number of cases reported annually between 1969 and 1980, while in the U.S.A. during the early stages of the vaccination programme (when proportions of each child cohort vaccinated were low) the trend was for an increase in CRS. Increasing the average age at vaccination under the U.S.A. policy simply acts to increase the level of coverage at which this policy is of greater benefit than that of the U.K. (Fig. 15). For example, if boys and girls were vaccinated at 7 years of age, the point at which the ratio $\hat{\rho}(a_1, a_2)$ is equal to that for the U.K. policy rises to 96% coverage. With the current U.S.A. age at vaccination of approximately 1 year, the critical level of immunization coverage, \hat{p} , which must

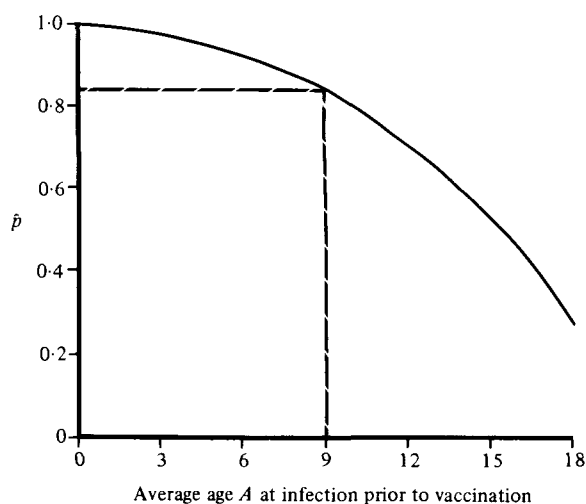


Fig. 16. Rubella. The critical level of immunization, \hat{p} , above which the U.K. policy has a greater impact on the incidence of C.R.S. than the U.S. policy, for various values of the average age at infection, A , prior to vaccination. ---, Current situation in the U.K. and U.S. where $A = 9$ years.

be exceeded if the U.S.A. policy is to have a greater impact than the U.K. policy in reducing the number of women of childbearing age at risk to infection is plotted in Fig. 16, for various values of A . Note that for an A value of 12 years, namely that assumed by Knox (1980) and Dietz (1981), the critical level of coverage is 70%. Our analysis, based on an average age of infection of 9 years, yields the higher figure of 84%.

Given the current levels of immunization in the U.K., which approach 80% by the age of 13 (see Fig. 11), vaccinating girls at age 12 is marginally better than the U.S.A. policy in reducing the value of $\hat{p}(a_1, a_2)$. Achieving high vaccine acceptance rates in Britain has proved difficult in the past, but if significant improvement over current levels were to occur then the U.S.A. policy would be of greater benefit. Acceptance rates in the U.S.A. are currently significantly higher than in the U.K. In 1980, for example, 96% of all children entering school in the U.S.A. were vaccinated against measles and rubella (CDC, 1982*a*). The predictions of our model therefore yield the satisfying conclusion that the U.K. policy is best for the U.K. and the U.S.A. policy is best for the U.S.A., given the current immunization levels in the two countries. A similar conclusion was arrived at by Hethcote (1983). However, as illustrated in Fig. 13, the U.S.A. policy had greater risks attached to it if acceptance rates decline significantly from the current levels.

Short-term dynamics

The steady-state results discussed in the previous section indicate what may happen (under the assumptions of our model) in the long term, for a given vaccination policy. As discussed earlier, however, the phrase 'long term' implies many decades after the instigation of the type of vaccination programmes employed in developed countries. The steady state would only be approached

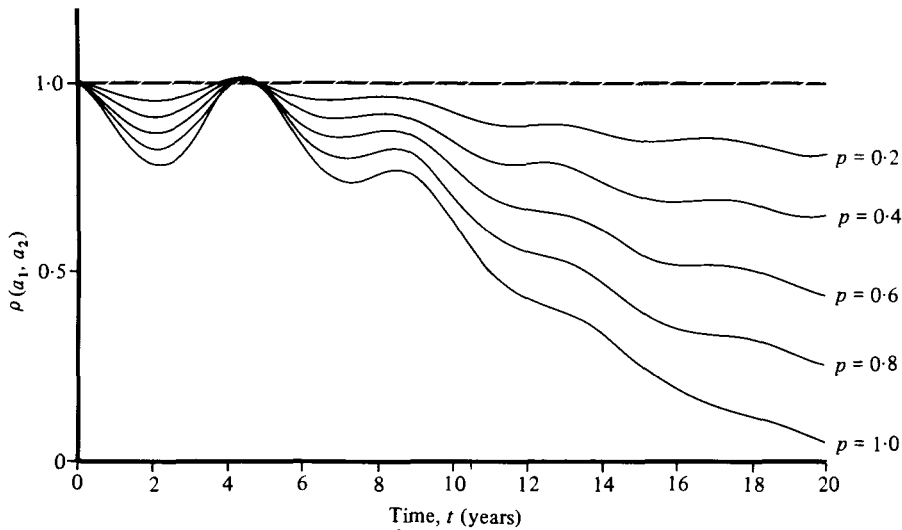


Fig. 17. Rubella. Temporal trends under the U.K. policy. Temporal changes in the ratio $\rho(a_1, a_2)$ are shown over a period of 20 years for five different levels of vaccination coverage ($p = 0.2, 0.4, 0.6, 0.8$ and 1.0). Parameter values are as follows: $A = 9$ years, $\bar{N} = 500000$, $L = 75$, $b = 12 \text{ yr}^{-1}$ (girls only), $a_1 = 16.0$ years, $a_2 = 40.0$ years. $\sigma = 34.76 \text{ yr}^{-1}$, $\gamma = 31.74 \text{ yr}^{-1}$, $X(0, t) = 6666.66$. The equilibrium densities of susceptibles and latents prior to vaccination were calculated as $\bar{X}^* = 59985.6$, $\bar{H}^* = 191.73$ and the force of infection was set at $\lambda = 0.111$ in the unvaccinated community.

rapidly if every age group in a community was immediately vaccinated (upon the instigation of control measures) in such a manner that the required level of herd immunity, p , was equal throughout all the age classes. In practice, vaccination programmes usually focus on selected age classes of a community, such as young children or 12-year-old girls in the case of the U.K. rubella programme. In these instances, many decades pass before the full effects of herd immunity are realized by the community.

We employed standard methods of numerical analysis to generate time-dependent solutions of the model defined by equations (3)–(6); the details are outlined in Appendix 4. This approach allowed us to calculate time-dependent changes in quantities such as the density of susceptibles of age a , $X(a, t)$, the net force of infection, $\lambda(t)$, and the ratio of cases after to before vaccination, $\rho(a_1, a_2)$, for both the U.K. and U.S.A. vaccination policies.

Taking the U.K. policy first (where girls, and only girls, are vaccinated at age 12 years), time-dependent changes in the ratio $\rho(a_1, a_2)$ (with $a_1 = 16$, $a_2 = 40$ years) are depicted in Fig. 17 for various levels of vaccination coverage, p . The results are of considerable interest. For all levels of vaccination coverage, the ratio initially falls in value as a result of the perturbation to the density of susceptibles within the population, but then recovers once the density of susceptibles rises as a consequence of the reduced net force of infection. The interval between the start of vaccination and the epidemic resurgence of infection is precisely the inter-epidemic period T for rubella of between 4 and 5 years. Different levels of vaccination have little influence on this period, since by vaccinating only 12-

year-old girls, only a small percentage of the total pool of susceptibles is initially immunized. Note, however, that this small percentage is enough to trigger a perturbation in the system which reduces the overall density below the critical value \bar{N}_T , for disease persistence, reduces the effective reproductive rate, R , to less than unity, and pumps oscillatory behaviour in disease incidence. The initial oscillation is sufficient to raise the ratio $\rho(a_1, a_2)$ slightly above unity at the end of the inter-epidemic period, for all values of p . Thereafter, however, the ratio is consistently below unity, as the number of cohorts of vaccinated 12-year-old girls increase and as they move into the childbearing age (16–40 years of age). Very minor oscillations still occur with a period of 4–5 years, but these will hardly be detectable given the accuracy of case notification records. The system takes a substantial period of time (more than 20 years) to approach the steady-state levels discussed in the previous section (see Fig. 13).

How well do the predicted patterns match the numbers of reported CRS cases since vaccination in the U.K. started in 1970 (see Fig. 12)? The answer is, remarkably well, given the simplicity of our model and the many problems of interpretation surrounding the reported case records (which were discussed earlier and considered in the legend to Fig. 12). The observed data records a peak in CRS incidence approximately 4–5 years after the initiation of vaccination. Thereafter the number of cases appears to decline. The level of immunization of yearly cohorts of 12-year-old girls since 1971 has been between 0.6 and 0.8, and hence these p value curves in Fig. 17 are the ones on which the comparison of observed and predicted should be made. One difference between Figs. 17 and 12 is that the predicted peak at 4–5 years appears higher than that observed. This may be because our model does not take account of the screening of pregnant women during antenatal care, nor of the number of pregnancies terminated as a result of rubella infection. Screening and termination have been used concomitantly with the vaccination of 12-year-old girls, and hence we would expect observed trends to decline more rapidly than our predictions.

Would any benefit accrue in the U.K. from vaccinating both boys and girls at age 12 years? As indicated in Fig. 18, our model suggests definitely not. In fact, the situation deteriorates when boys are also vaccinated, as this acts to reduce the force of infection within the community and thus reduces the number of girls who acquire protection by natural infection.

The U.S.A. policy of vaccinating both boys and girls between the ages of 1 and 2 years has very different effects on the temporal dynamics of rubella than does the U.K. policy. The predictions of our model are displayed in Figs. 19*a* and *b*, which illustrate temporal changes in the ratio $\rho(a_1, a_2)$ for different levels of immunization coverage, p . The perturbation to the net force of infection created by vaccinating boys and girls at an early age triggers marked oscillations in the incidence of infection and hence the ratio $\rho(a_1, a_2)$. These oscillations become progressively more pronounced as the level of immunization rises. Concomitantly the inter-epidemic period lengthens substantially (essentially because the simple, linearized estimate of T breaks down as nonlinear effects become more pronounced). For example, when p is 0.2, the period T is roughly 4–5 years. When p is 0.8 the period lengthens to 10–11 years. The qualitative agreement between observation (Fig. 9) and theory is again satisfactory given the simplicity of our model. For

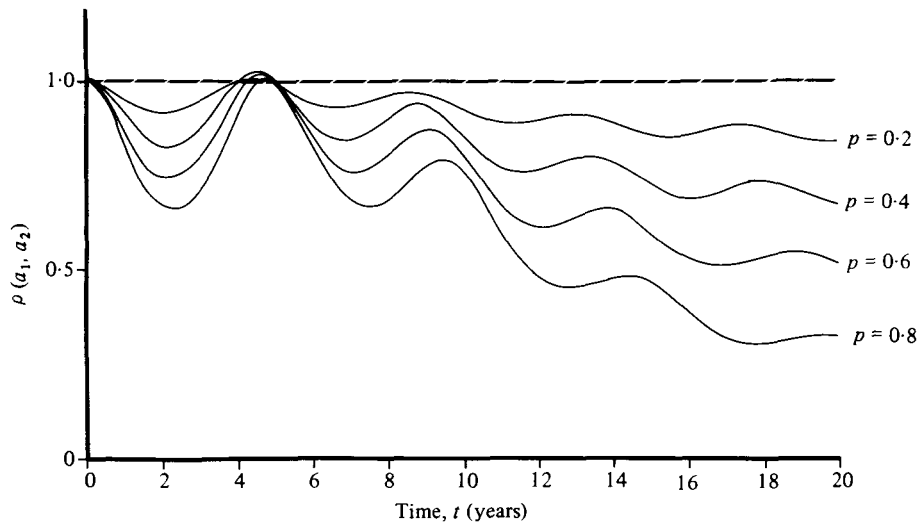


Fig. 18. Rubella. Identical to Fig. 17 but with the vaccination of boys and girls at age 12 years ($b = 12.0$). Parameter values as defined in the legend to Fig. 17.

instance, in Fig. 9 there is evidence of a 9-year fluctuation in the number of CRS cases under the impact of an immunization coverage roughly between 0.8 and 0.9, while our theory suggests a 10- to 11-year cycle. Note that during the peak phase of a predicted epidemic the ratio $\rho(a_1, a_2)$ rises substantially above unity. The observed trends in Fig. 9 do not match this prediction but here, as in the U.K. situation, the model does not take account of the screening and pregnancy-termination programme operating in conjunction with vaccination. Observed oscillatory trends are therefore likely to be less severe than the predicted patterns.

An additional discrepancy between our theory and the observations is that, with a 0.8 vaccination coverage, theory predicts very low numbers of CRS cases with the first 2–3 years after the start of control (before the numbers increase during the epidemic at 10–11 years after the start of vaccination). Observed patterns do not show such a marked and rapid decline, presumably because vaccine coverage rose gradually – not discontinuously – to the current figure of 0.96; this gradual increase occurred between 1970 and 1982. A further point to note is the time taken by the predicted trends to approach the steady-state levels. This time period is long and increases progressively as the level of vaccination coverage increases (Fig. 19).

The severity of the oscillations predicted by our model may appear contrary to intuition. This is not so, however, when one considers the severity of the perturbation to the net force of infection within the community, triggered by vaccinating a high proportion of a cohort of boys and girls many years before the age they would naturally acquire the infection in an unvaccinated community. This point is made pictorially in Fig. 20*a*, where temporal changes in the net force of infection, $\lambda'(t)$, are plotted over 20 years for both a U.K. policy with 0.8 coverage of 12-year-old girls, and a U.S.A. policy with 0.8 coverage of 1-year-old girls and boys. Note the marked differences between the two policies.

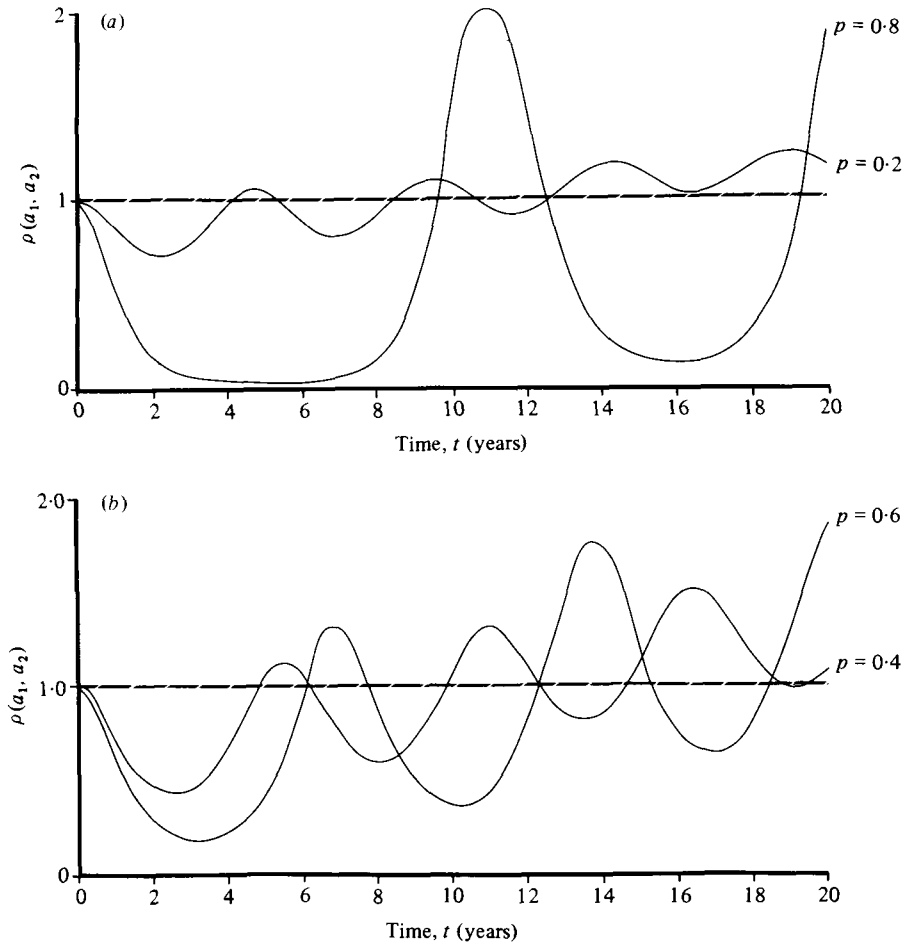


Fig. 19. Rubella. Temporal trends under the U.S. policy. Similar to Fig. 17 but with the vaccination of boys and girls at the age of 1 year ($b = 1.0$). (a), (b) Temporal changes under four different levels of vaccine coverage ($p = 0.2, 0.4, 0.6$ and 0.8). All other parameter values as defined in the legend to Fig. 17 ($a_1 = 16, a_2 = 40$).

A further illustration of this point is given in Fig. 20b, which records temporal changes in the ratio of the total number of rubella cases (over the age range 0–75 years) after and before vaccination. Two curves are shown, one for the U.K. policy and one for the U.S.A. policy, both with coverage levels of 0.8 (i.e. 80%). In accord with observed patterns (see Fig. 9), the U.S.A. policy has a much more marked impact on the total number of reported cases.

MEASLES: EMPIRICAL BACKGROUND

The epidemiology of measles has attracted wide attention partly as a result of the characteristic symptoms of this acute and highly communicable viral disease, which facilitate accurate clinical diagnosis. Mortality from measles in developed countries, resulting from respiratory or neurological causes, has been low over the

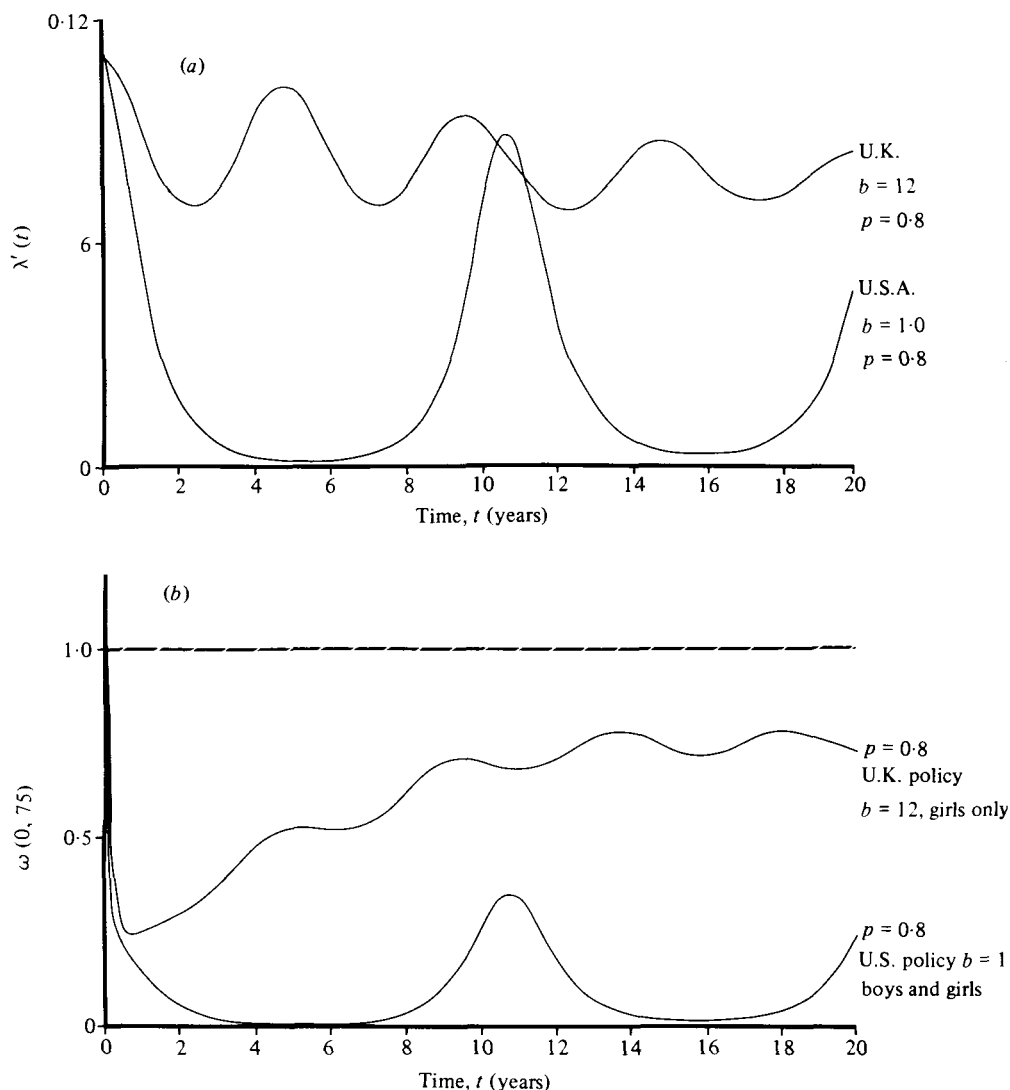


Fig. 20. Rubella. (a) A comparison of the differing impacts of the U.K. and U.S. vaccination policies on the force of infection $\lambda'(t)$. The vaccine coverage is set at 80% ($p = 0.8$) in both cases. The solid lines denote the U.K. and the U.S. policies. Parameter values as defined in the legend to Fig. 17. (b) Temporal changes in the ratio $\omega(0, 75)$ of the total number of rubella cases, $S(t)$, occurring between the ages of 0 and 75 years after vaccination divided by that before, under the U.S. and U.K. vaccination policies. Parameter values as defined in the legend to graph (a).

past 30 years (1 in 3000 to 1 in 5000 of notified cases) but morbidity is often high. The severity of measles is greatly influenced by the nutritional state of the child, and very high case fatality rates (sometimes as high as 20–30%) are observed in developing countries when malnutrition is rife. Measles is also thought to be a common cause of blindness in communities with vitamin A deficiencies, and to increase susceptibility to secondary infections as a result of its severe impact on the immune system of the patient.

Table 3. Average age, A , at which measles infection is typically acquired in different countries

Location	Time period	Average age, A (years)	Data base	Data source
England and Wales	1944–65	4.5–5.5	Case notifications	Registrar General's statistics
Various localities in North America	1912–28	4.0–6.0	Case notifications	Collins (1929)
Zambia, Rhodesia and South Africa	1960–8	3.0–4.0	Case notifications	Morley (1969)
Nepal (Terai)	1977	3.0–4.0	Serology	Davis (1982)
Ghana	1960–8	2.0–3.0	Case notifications	Morley (1969)
Eastern Nigeria	1960–8	2.0–3.0	Case notifications	Morley (1969)
India (Pondicherry area)	1978	2.0–3.0	Serology	Davis (1982)
Morocco	1960	2.0–3.0	Serology	Davis (1982)

Measles encephalitis occurs in approximately 1 of every 2000 reported cases in developed countries (CDC, 1982*b*). Survivors often have permanent brain damage and mental retardation. Measles during pregnancy is known to increase fetal risk.

The high morbidity resulting from measles, along with high prevalences of infection in large communities, promoted the widespread use of an attenuated measles vaccine in many developed countries when it became available in the mid-1960s.

Transmission of the infection is by droplet spread or direct contact, and the latent and infectious periods are approximately 7 days each (see Table 1).

The average age at infection, A

Measles is a highly infectious disease and, prior to immunization, in large communities few people went through life without experiencing the infection. In England and Wales in the 1950s, for example, at the age of 10 years roughly 95% of all children had experienced an attack.

The average age at infection, A , varies in different parts of the world depending on the prevailing social and environmental conditions. In general the value of A varies from 2–3 years of age in communities in Africa and India, to between 4 and 6 years of age in unvaccinated communities in developed countries (Table 3). In the U.K. and U.S.A. prior to vaccination, for example, the average age in urban communities was approximately 5 years of age (Anderson & May, 1982).

The interepidemic period, T

The incidence of measles characteristically fluctuates in developed countries both on a seasonal and a longer time scale. Before the advent of immunization, the longer period was typically 2–3 years in Europe and North America (see Anderson & May, 1982). With latent and infectious periods of approximately 7 days each (Table 1), and an average age at infection, A , of 5 years, the basic model (see equation (31)) predicts an inter-epidemic period, T , of 2–3 years; this figure agrees with that observed. In developing countries when an A value of 2 years of age, the theory predicts that major epidemics will occur every 1–2 years. This is indeed the case in many high-density communities with high birth rates.

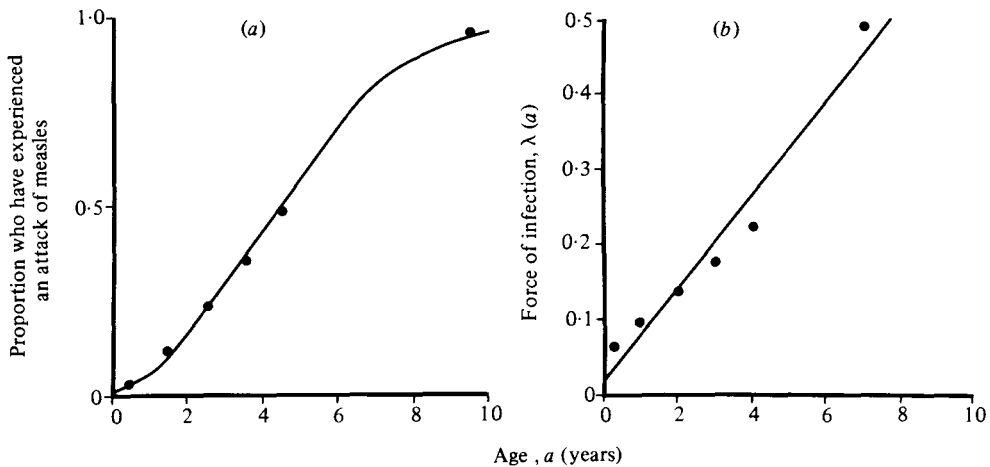


Fig. 21. Measles. (a) Proportion of children who had experienced an attack of measles at various ages in England and Wales in 1958 (based on case notification records). Observed values; —, predictions of a simple catalytic model with age-dependent rates of infection (see Appendix 2). (b). The age dependency in the rate or force of infection $\lambda(a)$. ●, Calculated values; —, best-fit linear model of the form $\lambda(a) = m + va$, where $m = 0.0178$ and $v = 0.063$ ($r^2 = 0.96$).

Maternal antibodies

Newborn infants are protected from measles infection by maternal antibodies for, on average, a 6-month period. Before widespread immunization in the U.K., nearly 100% of newborn infants had positive sera.

The force of infection

The force of infection, λ , tends to vary with age in Europe and North America. In the age range 0–10 years, the rate rises approximately linearly with age, presumably as a consequence of age-related changes in behavioural patterns (Griffiths, 1974; Anderson & May, 1982). An example of this trend is illustrated in Fig. 21.

Measles encephalitis: risk with age

The risk of measles encephalitis is known to vary with age. Age-specific data both for measles cases and for measles encephalitis cases in the U.S.A. are available for 1973–9. In this period, age was known for 151 of the 160 patients whose encephalitis cases were reported to the Center for Disease Control (CDC, 1981*b*). During the period 1973–5, the measles encephalitis to case ratio rose linearly with age (Fig. 22*a*). Similar data for England and Wales during 1980 are presented in Fig. 22*b*. The severity of the rise shown in the U.K. (Fig. 22*b*) is greater than that shown for the U.S.A. in Fig. 22*a*. However, the U.K. data in 1980 are based on only 58 reported cases of measles encephalitis. Some concern over these findings may arise from the observation that widespread immunization within a community tends to increase the average age, A , at which an infection is acquired. In our analyses of the impact of vaccination on the incidence of measles encephalitis,

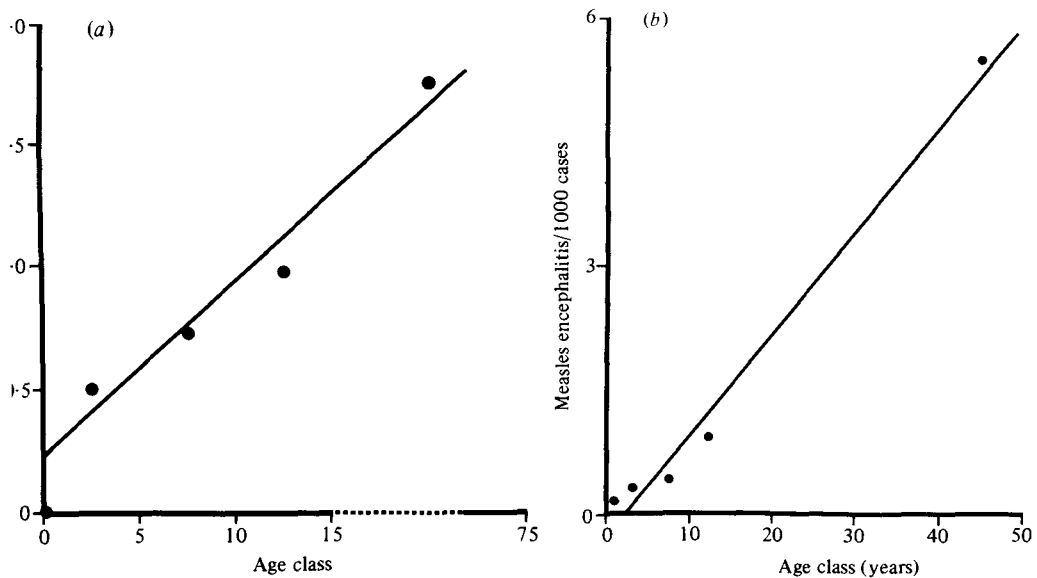


Fig. 22. Measles. (a) The age dependency in the ratio of measles encephalitis cases to 1000 measles cases in the U.S. between 1973 and 1975 (CDC, 1981*a*). ●, Observed values; —, best-fit linear model of the form $m(a) = c_1 + c_2a$, where $c_1 = 0.23$, $c_2 = 0.0717$ ($r^2 = 0.95$). (b) Identical to (a) but recording the case ratio for England and Wales in 1980 ($c_1 = -0.308$, $c_2 = 0.127$, $r^2 = 0.99$) (see text).

we define the measles encephalitis to case ratio displayed in Fig. 22 to be the age-related risk function, $m(a)$, for contracting serious disease from measles infection.

Vaccination policies in the U.S.A. and the U.K.

In the U.S.A., before measles vaccine was available, more than 400 000 measles cases were reported annually. Since the licensing of the vaccine in 1963, there has been a 99% reduction in the reported incidence of measles (in 1981 a total of 3032 cases were reported; CDC, 1982*a*); see Fig. 23. This high success rate is a direct consequence of the measles elimination initiative begun in 1978, whose primary aim was, and is, to achieve and maintain a very high percentage of herd immunity to measles in the U.S.A. A very high percentage of children are vaccinated before entering school, largely as a consequence of school immunization laws. These state laws require documentation of measles immunity at the time of entry into kindergarten or first grade. By January 1982 all 50 states enforced immunization laws and 96% of all children entering school in 1982 had been vaccinated (CDC, 1982*c*).

The recommended age for vaccination is 15 months, an age which is thought to maximize the rate of seroconversion (greater than 95%). Vaccination at an earlier age gives lower seroconversion rates as a consequence of the protection created by maternal antibodies. The average age at vaccination in the U.S.A. is currently between 1.5 and 2.5 years.

A notable consequence of the success of the U.S.A. programme has been a

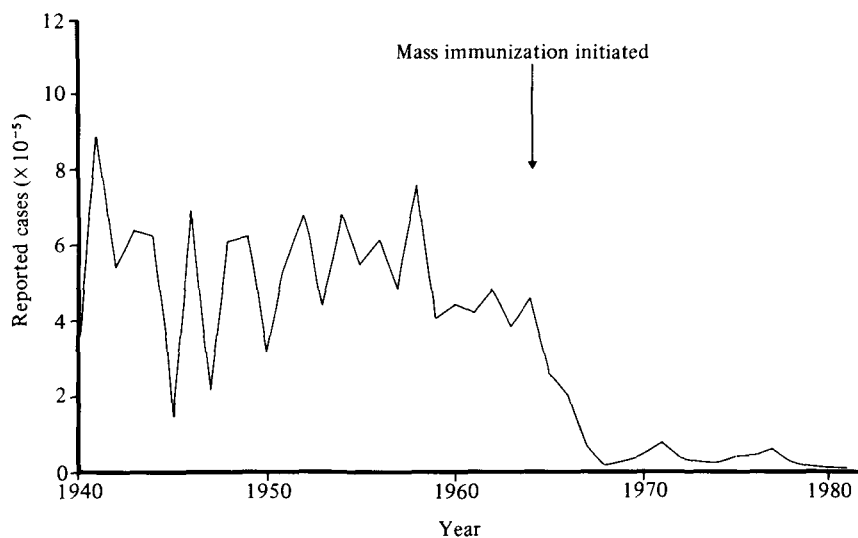


Fig. 23. Measles. Reported annual number of cases of measles in the United States between 1940 and 1981 (data obtained from Centers for Disease Control, U.S.A.).

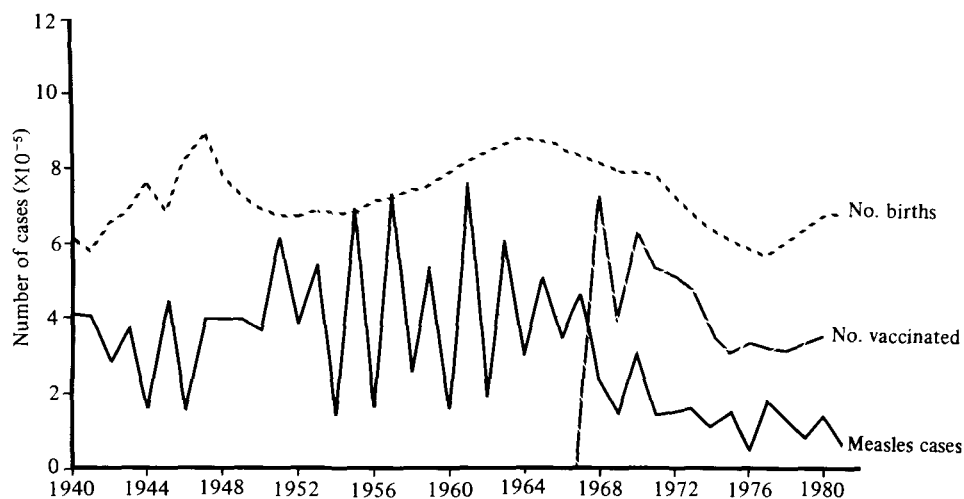


Fig. 24. Measles. Reported annual number of cases of measles in England and Wales during 1940–81, the number of live births, and the number of children vaccinated against measles each year (data from the Office of Population Censuses and Surveys, U.K., and the Department of Health and Social Security, U.K.).

marked increase in the average age at which those still susceptible acquire measles. Prior to vaccination the average age was around 5 years, while in 1980 more than 60% of cases occurred among persons over 10 years of age. More than 20% of reported cases were in the 15- to 19-year-old age group.

With the current strategy based on achieving and maintaining very high immunization levels, along with diseases surveillance and prompt measures to control outbreaks, it is hoped to be able to eradicate indigenous measles in the U.S.A. in the near future (CDC, 1982*d*).

The U.K. vaccination strategy is similar in design to that of the U.S.A. but much less effective due to low acceptance rates. Since the beginning of extensive immunization in 1967, acceptance levels have never exceeded 54% of a given yearly cohort of children; the proportion immunized has remained approximately constant over the past 15 years, remaining close to 50%. The average age at vaccination in the U.K. is currently 2.2 years. The choice of whether or not a child is vaccinated is left to the parents, under the guidance of their local doctor. The average age at infection, A , is currently around 5 years, a value which has changed little since immunization began. The number of cases reported annually has declined since 1967 (see Fig. 24), although epidemics still occur on a slightly lengthened period of approximately 3 years.

MEASLES: ANALYSIS AND MODEL PREDICTIONS

As was the case for rubella, this section is divided into two parts. The first considers the equilibrium state towards which a population converges under the influence of a particular vaccination programme. The second examines the epidemiological dynamics as the population approaches the steady state.

Our interest is in the impact of vaccination on the measles encephalitis to measles case ratio (see Fig. 22). At equilibrium, our assessment is based on the ratio $\hat{\rho}(a_1, a_2)$, which is defined as the number of cases of encephalitis in the age range 1–75 years after vaccination, divided by the number of cases occurring in the same age range prior to immunization. This ratio $\hat{\rho}$ is estimated by the methods outlined earlier, and set out more fully in Appendix 1.

Equilibrium or steady-state properties

Before considering the equilibrium ratio $\hat{\rho}(a_1, a_2)$, we briefly comment on the overall level of herd immunity required to eradicate measles. The proportion of the population, p , that must be immunized in order to reduce the effective reproductive rate of measles below unity may be calculated from equation (13). In a community in which life expectancy, L , is approximately 75 years (assuming a step-function survival curve; type *B* in Fig. 1) and in which the average age at infection, A , prior to immunization was roughly 5 years, the basic reproductive rate is approximately 15. This yields a critical p -value of approximately 93%. In other words, the level of herd immunity must exceed 93% to eradicate the disease or, alternatively, under steady-state conditions 93% of each yearly cohort of children must be immunized at or near to birth. If we take into account the fact that the actual average age at vaccination in the U.K. and the U.S.A. is nearer 2 years of age, as a consequence of low seroconversion rates in the first 12 months of life due to maternal antibodies, then we obtain a revised value of p of approximately 96% (using equation (32)). Thus if the average age at vaccination is roughly 2 years, then under steady-state conditions 96% of each yearly cohort of children must be immunized if measles eradication is the aim (Anderson & May, 1982). Recent experience in the U.S.A. lends some support to this estimate, although it must be remembered that the vaccine percentage efficiency is in the high-to-middle 90s, not 100%.

Turning to measles encephalitis cases, Fig. 25 shows the steady-state predictions

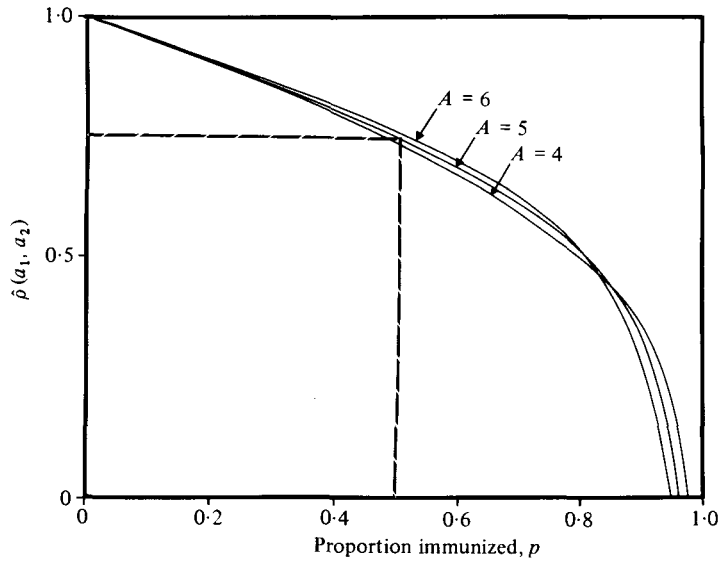


Fig. 25. Measles. The equilibrium ratio $\hat{\rho}(a_1, a_2)$ of measles encephalitis cases in the age range 0–75 years after vaccination of a proportion p at age b divided by the cases before vaccination (see Appendix 4). The age-dependent risk function $m(a)$ employed to calculate $\hat{\rho}(a_1, a_2)$ is as defined in Fig. 22(a), and we assume a type B survival function with a life expectancy of 75 years. Three curves are recorded for three different values of the average age A at infection prior to control ($A = 4, 5$ and 6). —, The current situation in the U.K., with a p value of approximately 0.5. The age at vaccination (b) was set at 2.0 years ($a_1 = 0, a_2 = 75.0$).

of our model (see Appendix 1) for varying levels of vaccination, p , and for 3 different values of the average age at infection, A , prior to vaccination. In the calculations of the ratio $\hat{\rho}(a_1, a_2)$ of cases after to cases before vaccination, as displayed in this figure, the average age at vaccination was set at 2.2 years, to match the current U.K. situation. Note that in Fig. 25 the proportion p at which the ratio $\hat{\rho}(a_1, a_2)$ is equal to zero (measles eradication) is given by equation (32) with a V -value of 2.2 years and the appropriate value of A . Note that we use the symbol V to denote the *average* age at vaccination; in our model calculations the symbol b denotes the age at vaccination where it is assumed that all vaccination occurs at precisely age b .

The important point to note from Fig. 25 is that vaccination, at whatever level, always acts to reduce the number of encephalitis cases (given the form of the measles encephalitis cases to measles cases risk ratio documented in Fig. 22a). However, the reduction in the number of cases is nonlinearly related to the proportion of a cohort immunized. For example, taking parameter values appropriate to the U.K. situation (i.e. $A = 5$ years, $V = 2.2$ years, $p = 0.5$), we see that immunization levels of 50% result in only a 25% reduction in the number of encephalitis cases. A 90% coverage results in a 75% reduction, while higher levels of vaccination result in eradication. The nonlinear effect is important, because substantial reductions in the number of cases of encephalitis will only occur as the overall level of herd immunity begins to approach the critical level for eradication. Again experience in the U.S.A. lends some support to this prediction.

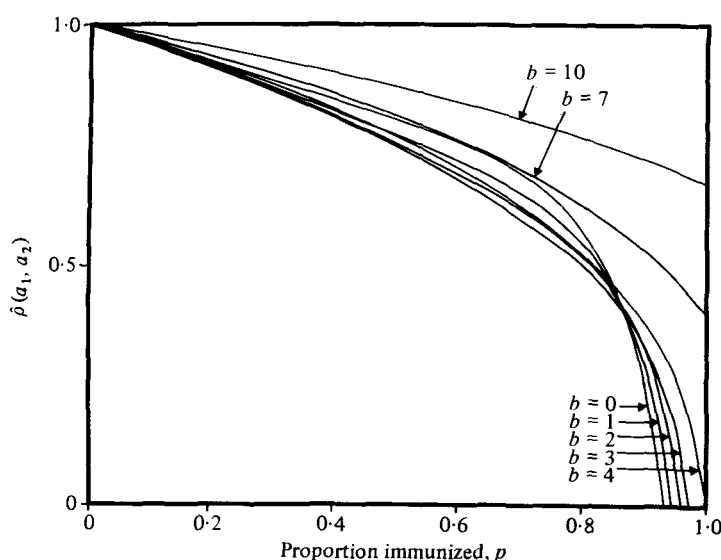


Fig. 26. Measles. Identical to Fig. 25 but with A fixed at 5 years. The various lines record changes in the ratio $\hat{\rho}(a_1, a_2)$ for seven different ages at vaccination ($b = 0, 1, 2, 3, 5, 7$ and 10 years) ($a_1 = 0, a_2 = 75$).

A final point of interest concerns the effects of changes in the average age, V , at which children are vaccinated. The influence of various values of b on the ratio $\hat{\rho}(a_1, a_2)$ is depicted in Fig. 26. There are two major constraints on changing the value of V . For practical reasons, associated with the effects of maternal antibodies on sero-conversion rates following vaccination, V cannot be less than 1.25 years. In addition, if the average age of vaccination, V , is greater than the average age at which the infection was acquired prior to vaccination, A , the infection can never be eradicated (see equation (32) and Anderson & May, 1982). In between these limits $V = 1.25\text{--}5.00$ years; a small benefit accrues from keeping V as close as possible to the lower bound of 1.25 years (Fig. 26).

Short-term dynamics

Our interest in this section is not to contrast two different vaccination policies, but simply to examine the temporal behaviour of measles in populations vaccinated at different levels of coverage. Following the actual practice in the U.K. and U.S.A., we assume that the average age at vaccination of boys and girls is 2 years and consider immunization coverages (the value of p) of 20%, 40%, 60% and 80%. As before, we measure the impact of vaccination on the ratio of encephalitis cases after to cases before vaccination. The results of our numerical solutions over a period of 20 years are presented in Fig. 27. The first point to note is that vaccination at any level of coverage lowers the ratio $\hat{\rho}(a_1, a_2)$ to below unity. This situation is to be contrasted with that discussed in the previous section for CRS. The second point concerns the inter-epidemic period, which before the advent of immunization was about 2–3 years (given an average age at infection of 5 years). Vaccination acts to lengthen the period progressively as the coverage increases. Note, however, that the period lengthens slowly over a 20-year span, as more and

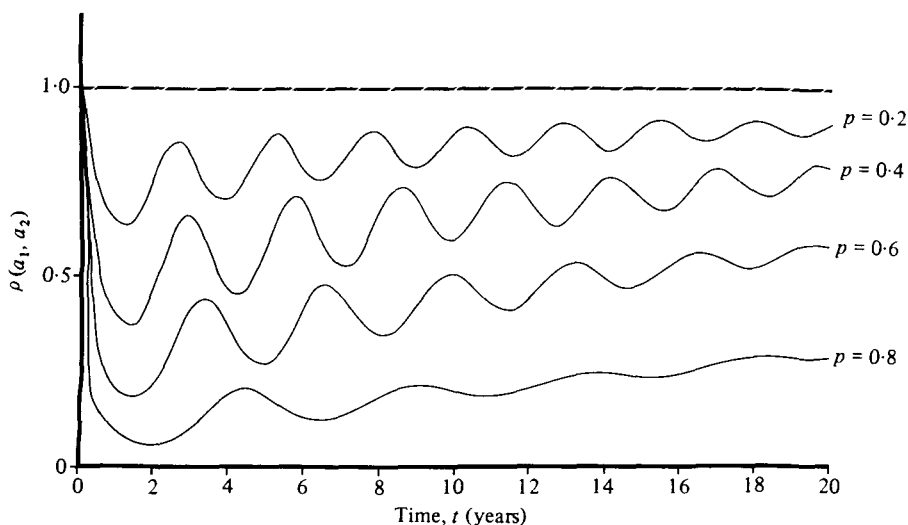


Fig. 27. Measles. Temporal trends. Temporal changes in the ratio $\rho(a_1, a_2)$ are shown for four different levels of vaccination coverage ($p = 0.2, 0.4, 0.6$ and 0.8). Parameter values are as follows: $A = 5$ years, $\bar{N} = 500000$, $a_1 = 0.0$ years, $a_2 = 75.0$ years, $\sigma = 52.14 \text{ yr}^{-1}$, $\gamma = 52.14 \text{ yr}^{-1}$, $L = 75$ years, $X(0, t) = 6666.66$. The equilibrium densities of susceptibles and latents prior to vaccination were calculated as $\bar{X}^* = 33333.33$, $\bar{H} = 127.85$, and the force of infection was set at $\lambda = 0.2$ in the unvaccinated community.

more cohorts of children are exposed to vaccination. This result is of some interest, since one criticism of simple theoretical models is that at equilibrium they predict longer inter-epidemic periods under moderate to high levels of vaccination coverage than those observed, for example, in the U.K. Our analysis of temporal behaviour, however, shows that given the situation in the U.K., where the average cohort coverage is between 0.4 and 0.55 (see Fig. 28), over the first 14–15 years of vaccination the inter-epidemic period will only lengthen to a value of around 3 years (Fig. 27). This prediction accords with observed events (Fig. 24).

At high levels of vaccine coverage, such as those achieved in the U.S.A., our model suggests a more rapid lengthening of the inter-epidemic period; at a p -value of 0.9 the cycle would be approximately 6–7 years, although of small amplitude. Observed patterns in the total number of reported measles cases in the U.S.A. (see Fig. 23) lend some support to this prediction. These observed trends suggest a lengthening of the inter-epidemic period from between 2–3 years prior to vaccination to roughly 6–8 years in the period 1964–80 (Fig. 23). The numerical results displayed in Fig. 27 suggest that 20–30 years must pass after the initiation of mass immunization before the equilibrium state (corresponding to Figs. 25 and 26) is attained. A further point of interest in the models is the tendency for the amplitudes of the oscillations in disease incidence to be reduced as vaccination coverage increases. This theoretical finding is again in agreement with the patterns observed in the U.K. and U.S.A., where currently the seasonal peaks in incidence are virtually as apparent as the multiple-year cycles (see also Fine & Clarkson, 1982a).

Our model can also be employed to examine temporal changes in the annual

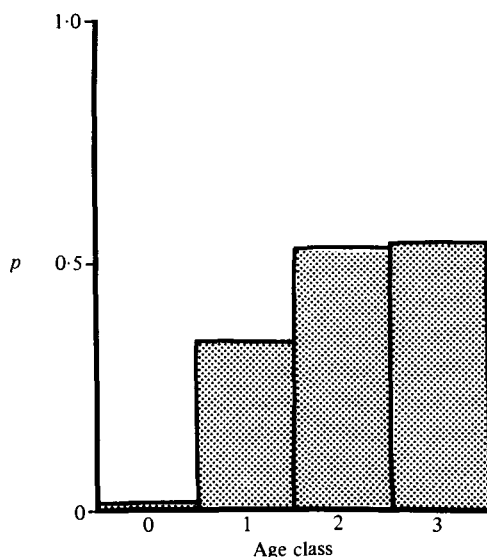


Fig. 28. Measles. The proportion p of boys and girls in England who were immunized against measles infection by the end of 1980 in the age range 0–3 years (data from the Department of Health and Social Security, U.K.).

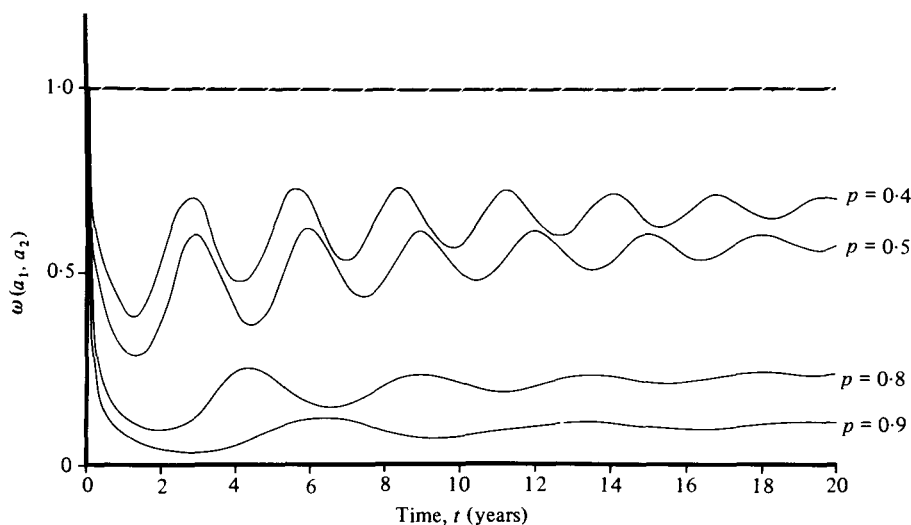


Fig. 29. Measles. Temporal changes in the ratio $\omega(a_1, a_2)$ of the total number of measles cases, $S(t)$, occurring between the ages of 0 and 75 years after vaccination divided by that before. Changes are recorded for four different levels of vaccination coverage ($p = 0.4, 0.5, 0.8$ and 0.9). Parameter values are as defined in the legend to Fig. 27.

number of cases in vaccinated communities (in our model, population size \bar{N} was set at 500 000), as opposed to the number of measles encephalitis cases. We again look at the ratio of annual numbers of cases after vaccination (in the age range 0–75 years) divided by the average number of annual cases before control (the equilibrium state of the unvaccinated community). The results are shown in Fig. 29 for coverage levels of 0.4 and 0.5 (to reflect the U.K. situation) and 0.8 and 0.9

(to reflect the U.S.A. situation). These predictions are in broad agreement with the observed trends shown in Figs. 23 and 24, with the qualification that the observed trends are created by gradually increasing vaccination coverages.

FUTURE RESEARCH

The qualitative agreement between observation and the predictions of our model is surprisingly good, given the simplicity of the latter. There are, however, several ways in which the next generation of models can incorporate refinements that give a better representation of known biological detail. In this section we mention five factors which, in our view, require greater attention; the first four concern the structure and analysis of the models, while the fifth deals with data collection.

(1) Our model contains the assumption that the force of infection, λ , is independent of age. For most common viral and bacterial infections of childhood this assumption is false: there is a general tendency for the rate of infection to increase during early childhood (often linearly, as in the case of measles (see Fig. 21)); to reach a peak in the early teens; and to decline thereafter. We took account of these trends in our estimation of an average force of infection from all age classes and in the calculation of the average age at infection. We did not, however, represent λ as a function of age in the model but simply employed the average value for all age classes. The effects of incorporating age dependence in this parameter λ should be explored, although there are difficulties in determining how vaccination influences this age dependence. We believe such modifications will not alter our qualitative conclusions but will influence quantitative detail. In particular, we suspect that the inclusion of a force of infection which rises over the first 10 years of life will act to decrease the predicted impact of vaccination on the inter-epidemic period (T) and on the average age of infection (A). This suspicion is borne out by some preliminary numerical studies, but much remains to be done.

(2) Our model contains the assumption (widely made in mathematical epidemiology), that the population mixes in a homogeneous manner: at a given point in time, each susceptible has an equal probability of encountering an infectious person. We weaken this assumption to some extent (the 'weak homogeneous mixing assumption') by representing the net rate of acquisition of infection in our model as the product of the force of infection times the density of susceptibles of given age at a given point in time, where the force of infection in an unvaccinated community is estimated from empirical information. In natural communities, however, there will clearly be groups of individuals who are less at risk of exposure to infection than other groups. Children living in isolated rural communities and attending local schools with small total attendance are an example. None the less, we believe that for countries such as England and Wales the use of average probabilities of contact under a homogeneous mixing assumption is a reasonably good approximation to observed events, at least in communities such as cities and large towns or for the total population of the country. The qualitative agreement between theory and observation lends support to this belief. Even in a country as large as the U.S.A., it is remarkable that prior to vaccination, taking the country as a whole, case reports of measles (for example) illustrate a two- to three-year

cycle in abundance. In spite of these observations, however, there is clear need for further work to examine the impact of heterogeneous mixing on the dynamics of directly transmitted infections. Some progress has recently been made, but more data-oriented mathematical studies are required (Hethcote, 1978).

Similar comments also apply to vaccination coverage, since this is rarely uniform throughout the different health regions of a country. The epidemic of measles in El Paso, U.S.A., during the period March–June 1981 is a good illustration of this point. In the Ysleta Independent School District, which has the highest attack rate, only 65% of the students were immune to measles. Taking the U.S.A. as a whole in the same period, more than 90% of schoolchildren were protected against measles infection (CDC, 1982c). Attaining uniform vaccine coverage throughout a country will always be difficult, and this problem could shed some doubt on the likelihood that indigenous measles will eventually be eradicated from the United States. Vaccine acceptance rates in the U.K. also vary among different localities, depending on local public health policy (Fine & Clarkson, 1983).

(3) Our analyses of measles and rubella is based on the assumption that the respective vaccines confer lifelong immunity against re-infection. This appears, for the vast majority of individuals, to be the case for measles, but doubts have been expressed about the long-term efficacy of rubella vaccines. Since the rubella vaccine was only licensed in 1969, it is probably too early to be able accurately to assess its long-term properties. The epidemiological trends observed so far, however, do not suggest any serious loss in immunity in vaccinated individuals (Preblud, Serdula & Frank, 1980). If firm evidence of loss of immunity is produced, further research is required to modify the existing framework of our model.

(4) As indicated earlier in this paper, very few mathematical studies of either epidemic or endemic infections have explored the kinds of temporal changes in the densities of susceptibles and infecteds that can be brought about by control policies (such as vaccination) or by other factors (such as changes in the net birth rate within a community). The work outlined above suggests that more attention should be devoted to this area, particularly when predictions are to be compared, as they always should be, with observed patterns. In any such work, the accuracy and appropriateness of the numerical methods used to generate sequences of temporal changes must be carefully understood. As discussed earlier, this point may be illustrated by comparing our results with those reported by Knox (1981) and Cvjetanovic *et al.* (1982). Immunization on a very large scale is a relatively recent phenomenon, and country-wide vaccination programmes against many common viral and bacterial infections are currently only in their second or third decade of operation. To compare events before and immediately after the advent of mass immunization, equilibrium properties of models of disease dynamics are of limited use.

(5) Theory and observation clearly indicate that temporal changes in disease incidence are associated with the changes in the average force of infection within a community. Measurement of this parameter, along with related ones such as the average age at vaccination, can best be achieved by means of serological studies that record the decay with age in the proportion susceptible to a specific infection. Estimates can be obtained from case notification records, but these are notoriously unreliable. We echo the plea made recently by Grist, Reid & Young (1981) for more

detailed serological data based on surveys carried out before and during the course of a vaccination programme. Such information is of obvious practical value to public health authorities (for example, in confirming rates of vaccine acceptance), but it also provides a basis for testing theoretical predictions and the associated biological assumptions incorporated in mathematical models.

CONCLUSIONS

The analyses presented in this paper suggest that herd immunity does not always act to the advantage of the individual. Complications can arise when the risk of serious disease increases with age, and are a consequence of the tendency of mass immunization to raise the average age at infection above the value pertaining prior to control; individuals in the older (or childbearing) high-risk age classes may thus have a greater chance of acquiring infection after the advent of vaccination than before.

For rubella, we predict that this situation will arise for women of childbearing age if vaccine coverage is less than 55%, when boys and girls are vaccinated around one year of age (Fig. 13). We suggest that the U.K. policy of vaccinating girls, and only girls, at around 12 years of age will always result in a greater reduction in CRS cases than the U.S.A. policy of vaccinating girls and boys at around one year of age, provided vaccine acceptance rates are less than 84%. Above this level the U.S.A. policy will be more beneficial. Since acceptance rates are currently below 84% in the U.K. and above 84% in the U.S.A., we are drawn to the conclusion that the British policy is currently best for Britain and the U.S.A. policy best for the United States. In the U.K., however, acceptance rates have been steadily rising since 1974, and currently 80% of all 12-year-old girls are immunized. Our analyses suggest that, if such improvements continue, the U.S.A. policy will, *in the long term*, have a greater impact in reducing the incidence of CRS. In the short term, however, note that the U.S.A. policy has a tendency to induce oscillations in the incidence of CRS (Fig. 19), the period between peaks depending on the level of vaccine coverage. At high levels of coverage (greater than 84%) we predict the interval will be 10–12 years or more. The U.K. policy, on the other hand, is unlikely to induce severe oscillations in incidence, and high vaccine coverage levels will do little to lengthen the natural 4- to 6-year cycle of rubella incidence (Fig. 17). The possibility that marked fluctuations in CRS incidence may be induced under the U.S.A. policy will be substantially reduced by careful screening of women during antenatal care and the vaccination of non-pregnant susceptible women in the childbearing age classes. Such measures are currently in operation in the U.K. and U.S.A. and have resulted in a significant number of terminations as a consequence of contact with rubella during pregnancy (Fig. 30).

In the case of measles encephalitis, even low levels of vaccination act to reduce the incidence (Fig. 27). Our results suggest, however, that the relationship between vaccination acceptance rate and disease incidence is nonlinear, with the consequence that substantial improvements will occur only at high levels of coverage. Currently, high acceptance rates have been achieved in the U.S.A. but not in the U.K. (Figs. 23 and 24). It would seem prudent in the U.K. to attempt to improve the level of childhood vaccination against measles infection.

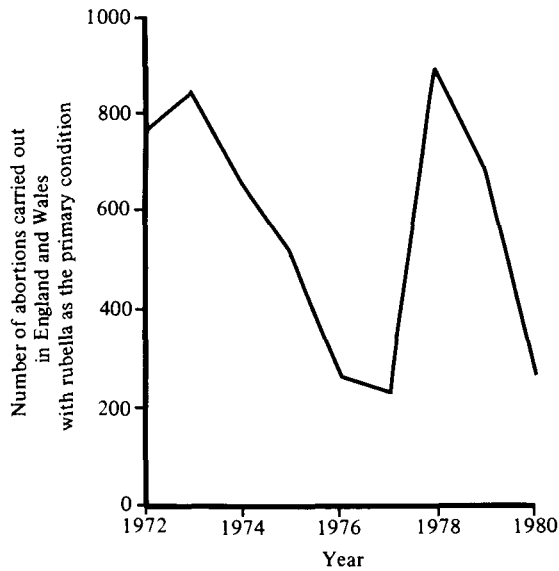


Fig. 30. The number of abortions in England and Wales carried out each year from 1972 to 1980, in which rubella is mentioned as a primary condition. Note the two peaks with a 5-year interval between them, created by the rubella epidemics in England and Wales in 1973 and 1978 (unpublished data supplied by Dr W. C. Marshall, The Hospital for Sick Children, Great Ormond Street, London).

Herd immunity is a topical issue in the U.K., largely due to the current epidemic of pertussis which appears to be a consequence of the recently lower levels of vaccination (resulting mainly from suggestions that vaccination may, under certain circumstances, result in serious neurological disease; H.M.S.O., 1981). We do not address the issue of pertussis incidence and vaccination in this paper, but it should be noted that for most common viral and bacterial infections of children, and in particular measles, rubella and pertussis, the risk of acquiring infection will tend (in both vaccinated and unvaccinated communities) to oscillate in value as a consequence of oscillations in disease incidence. Any assessment of average risk must therefore be based on many years' data, with the number of years depending on the average inter-epidemic period. The predicted effect of high levels of vaccination on the incidence of CRS under the U.S.A. policy (see Fig. 19) is a good illustration of this point. In certain years, even with an 80% vaccination coverage level, the risk of a mother acquiring rubella infection will be high. On average, however, over a 20-year period the risks will be substantially less in a vaccinated community than in an unvaccinated one. The issue of risk assessment for infectious diseases is a subject which requires much more attention than it has received in the past. Such assessments are, in practice, complicated by social and psychological factors, which often result in perceived risks differing widely from the actual statistical risks (see, e.g., Starr & Whipple, 1980).

Finally, we wish to urge the belief that simple mathematical models for disease dynamics can be helpful tools in the design of public health policy, provided they are used sensibly. Many people have rightly criticized models that pursue the

mathematics for its own sake, making only perfunctory attempts to relate the findings to epidemiological data; despite earnest efforts, our own work is undoubtedly open to this criticism. But there is a converse danger which is less widely appreciated: the complexities of herd immunity are such that years of clinical experience and the most refined intuition will not always yield reliable insights into the dynamical trajectories or long-term consequences of a specific vaccination programme. Moreover, insensitive use of a computer will not always solve these problems, for (as we have seen) if a computer is given inappropriate instructions it will usually give inappropriate answers. What is needed, in our view, is collaboration between people who really understand the epidemiological data and people who really understand the mathematics, with the mathematical models being founded on data and with their predictions being tested against available facts. We hope that our moderate success in confronting simple age-structured models with observed epidemiological data for rubella and measles may advance this cause.

We gratefully acknowledge John Cradock-Watson for the provision of unpublished data on rubella serology, John Pattison and Mary Anderson for many helpful discussions and Janet Manners and Chris Hewitt for general assistance and the preparation of the figures and typescript. We further acknowledge the Department of Health and Social Security, the Office of Population Censuses and Surveys, the Public Health Laboratory Service (in England, Wales and Ireland), the Centres for Disease Control (U.S.A.) and Dr Marshall at Great Ormond Street Hospital for Sick Children for the provision of records and statistics of disease incidence. This work was supported in part by the U.S. National Science Foundation, under grant DEB 81-02783.

APPENDIX 1

This appendix concentrates mainly on equilibrium results. We begin by considering the steady state without vaccination, and then examine the corresponding steady states under various vaccination programmes. The ratios \hat{w} and $\hat{\rho}$ can be calculated directly from these results. The appendix also outlines how maternal antibodies modify the calculations, and it ends with some remarks on the dynamics of the aggregated variables $\bar{X}(t)$, $\bar{Y}(t)$, etc. Some of the formulae have been discussed in detail by other authors, and some are new; we aim to present just enough detail for people to be able to repeat or extend the results that we present (usually graphically) in the main text.

Equilibrium age distributions

The equilibrium limit of equations (3)–(6) may be obtained by dropping all time dependences, to arrive at the set of ordinary differential equations:

$$dX/da = -(\lambda + \mu(a)) X(a), \quad (1.1)$$

$$dH/da = \lambda X - (\sigma + \mu(a)) H(a), \quad (1.2)$$

$$dY/da = \sigma H - (\gamma + \mu(a)) Y(a), \quad (1.3)$$

$$dZ/da = \gamma Y - \mu(a) Z(a), \quad (1.4)$$

$$dN/da = -\mu(a) N(a). \quad (1.5)$$

Here, and elsewhere, the age dependence can be factored out by introducing a new set of 'starred' variables,

$$X(a) \equiv X^*(a) \phi(a), \tag{1.6}$$

and so on. Here $\phi(a)$ is defined as

$$\phi(a) \equiv \exp \left[- \int_0^a \mu(s) ds \right]. \tag{1.7}$$

These starred variables, $X^*(a)$, etc., obey equations identical to (1.1)–(1.5), except that the terms involving $\mu(a)$ are no longer present. This set of simple, linear, differential equations, now with constant coefficients (λ is taken to be independent of age throughout these studies), are easily solved; see, e.g., Dietz (1975) or Bailey (1975). We give here only the results for the number of susceptibles (which gives equation (17) in the main text), and for the total population, of age a :

$$X(a) = N(0) \exp (-\lambda a) \phi(a), \tag{1.8}$$

$$N(a) = N(0) \phi(a). \tag{1.9}$$

The total number of susceptibles, \bar{X} , is obtained by integrating over all ages, equation (1).

For *type A survival* ($\mu = \text{constant} = 1/L$), we have $\phi(a) = \exp (-\mu a)$, and thence

$$\bar{X} = N(0)/(\lambda + \mu). \tag{1.10}$$

The corresponding total population is

$$\bar{N} = N(0)/\mu. \tag{1.11}$$

The net fraction who are susceptible at equilibrium is then

$$\hat{x} = \mu/(\mu + \lambda). \tag{1.12}$$

Equation (12) thus yields for R_0 the expression

$$R_0 = 1 + (\lambda/\mu). \tag{1.13}$$

Equations (19) and (20) of the main text follow from equation (1.13) and the identifications $\mu = 1/L$ (by definition) and $\lambda = 1/A$ (see Appendix 2).

Similarly, for *type B survival* ($\mu = 0$ for $a < L$, $\mu = \infty$ for $a > L$), we have $\sigma(a) = 1$ for $a < L$ and infinite thereafter, whence

$$\bar{X} = N(0) [1 - \exp (-\lambda L)]/\lambda, \tag{1.14}$$

$$\bar{N} = N(0)L. \tag{1.15}$$

The equilibrium fraction who are susceptible is thus

$$\hat{x} = [1 - \exp (-\lambda L)]/(\lambda L). \tag{1.16}$$

In conjunction with equation (12), this gives equation (21) for R_0 ; the equivalent equation (22) for R_0 follows from the identification $\lambda = 1/A$.

Clearly the Gompertz or *type C survival* function, or any other expression for $\mu(a)$, can be substituted into equation (1.7), and the values of \bar{X} , \bar{N} , \hat{x} and R_0 then computed along the above lines.

The above expressions for R_0 can alternatively be calculated by studying the equilibrium solutions of the differential equations for the total population variables, $\bar{X}(t)$, etc., as discussed below. This, indeed, is the usual derivation (e.g. Dietz, 1975, 1982). The above derivation is, however, simpler yet just as rigorous (being underpinned by Nold's (1979) formal and general proof that the effective reproductive rate is unity at equilibrium).

Equilibrium after immunization

Let the vaccination schedule be described by some age-specific rate, $c(a)$, at which susceptibles are successfully immunized. At equilibrium, the starred variables – with mortality factored out, equation (1.6) – will now obey

$$dX^*/da = -(\lambda' + c(a)) X^*(a), \quad (1.17)$$

$$dH^*/da = \lambda' X^* - \sigma H^*(a), \quad (1.18)$$

$$dY^*/da = \sigma H^* - \gamma Y^*(a), \quad (1.19)$$

$$dZ^*/da = \gamma Y^* + c(a) Z^*(a). \quad (1.20)$$

Here λ' is the force of infection at equilibrium, after the immunization programme is established.

Again, the integration of this set of equations (with the boundary conditions $X^*(0) = N(0)$ and $H^*(0) = Y^*(0) = Z^*(0) = 0$) is straightforward. The number of susceptibles of age a is now

$$X(a) = N(0) \exp\left(-\lambda'a - \int_0^a c(s) ds\right) \phi(a). \quad (1.21)$$

$N(a)$ is still given by equation (1.9). By integrating equation (1.21) for $X(a)$ over all ages, we can compute \bar{X} for any specified vaccination programme, $c(a)$, and mortality rate, $\mu(a)$; thence \hat{x} and R_0 can be obtained. We now present results for some special cases which arise in the main text.

(1) *Proportion p vaccinated at birth.* Here the vaccination rate, $c(a)$, is a discontinuous function, which can be treated by standard techniques (Dietz, 1981; Wickwire, 1977). Alternatively, we can observe that, in effect, $X(0) = (1-p)N(0)$. In either event, for this special case equation (1.21) becomes

$$X(a) = (1-p) N(0) \exp(-\lambda'a) \phi(a). \quad (1.22)$$

Here $N(a)$ still obeys equation (1.9).

For *type A survival*, equation (1.22) leads to the expression

$$\bar{X} = (1-p) N(0)/(\lambda'/\mu). \quad (1.23)$$

and thence

$$\hat{x} = (1-p)\mu/(\lambda' + \mu), \quad (1.24)$$

$$R_0 = (\lambda' + \mu)/[\mu(1-p)]. \quad (1.25)$$

With $\mu = 1/L$, equation (1.25) gives equation (33) which is discussed in the main text.

For *type B survival*, similar calculations give

$$\bar{X} = (1-p) N(0) [1 - \exp(-\lambda'L)]/\lambda'. \quad (1.26)$$

Thence, recalling that R_0 is the reciprocal of \hat{x} , equation (12), we have

$$R_0 = \frac{\lambda' L}{(1-p)[1-\exp(-\lambda' L)]}. \tag{1.27}$$

This gives equation (34) for R_0 , as discussed in the main text.

(2) *Proportion p vaccinated at age b .* Here, again, either $c(a)$ can be treated as a relative of the Dirac δ -function (being zero everywhere except at age b , where it is infinite), or we can observe that a fraction p of susceptibles of age exactly b are removed. Either way, we obtain the result

$$\begin{aligned} X(a) &= N(0) \exp(-\lambda' a) \phi(a) \quad (a \leq b) \\ X(a) &= (1-p) N(0) \exp(-\lambda' a) \phi(a) \quad (a > b) \end{aligned} \tag{1.28}$$

For *type A survival*, equation (1.28) leads to

$$\bar{X} = N(0) [1 - p \exp(-(\lambda' + \mu)b)] / (\lambda' + \mu). \tag{1.29}$$

\bar{N} is still given by equation (1.11), whence an expression for \hat{x} follows. From equation (12) we then have

$$R_0 = \frac{1 + (\lambda' / \mu)}{1 - p \exp(-(\lambda' + \mu)b)}. \tag{1.30}$$

This equation (1.30) links the parameters R_0 , p and b to λ' .

For *type B survival*, equation (1.28) gives

$$\bar{X} = N(0) [1 - p \exp(-\lambda' b) - (1-p) \exp(-\lambda' L)] / \lambda'. \tag{1.31}$$

Using equation (1.15) for \bar{N} , we get an expression for \hat{x} , and then via equation (12)

$$R_0 = \lambda' L / [1 - p \exp(-\lambda' b) - (1-p) \exp(-\lambda' L)]. \tag{1.32}$$

Some general observations can be made here. First, notice that equations (1.25) and (1.27) are indeed obtained from equations (1.30) and (1.32), respectively, in the limit $b \rightarrow 0$. Secondly, it is clear that more complicated age-specific vaccination schedules can be handled in the same way, even though the computations may be messier. Thirdly, if a proportion p of *girls only* is vaccinated at age b , the above results need only be modified by replacing p with $p/2$; the proportion of the total population that is vaccinated is simply $p/2$ (assuming a 1:1 sex ratio of girls to boys). This is an important point in connexion with the U.K. vaccination scheme against rubella.

(3) *Proportion p vaccinated at a constant rate c .* In this case, a fraction $(1-p)$ of the population are never vaccinated, while the remaining fraction p undergo vaccination at the constant per capita rate c ; the average age at vaccination for that fraction who are indeed vaccinated is $V = 1/c$. Here equation (1.21) gives

$$X(a) = N(0) [p \exp(-(\lambda' + c)a) + (1-p) \exp(-\lambda' a)] \phi(a). \tag{1.33}$$

For *type A survival*, equation (1.33) leads to

$$\bar{X} = N(0) \left[\frac{p}{\lambda' + c + \mu} + \frac{1-p}{\lambda' + \mu} \right]. \tag{1.34}$$

\bar{N} is, as ever, given by equation (1.11), and thence

$$R_0 = [(\lambda' + \mu)(\lambda' + \mu + c)] / [\mu(\lambda' + \mu + c - pc)]. \tag{1.35}$$

For given values of R_0 , μ , c and p , the force of infection λ' can be determined from equation (1.35). The critical condition for eradication of the infection corresponds to the limit $\lambda' \rightarrow 0$. Thus, using equation (1.35) in conjunction with equation (1.13) for R_0 , we find this critical level of vaccination to be

$$p > (1 + \mu/c)(1 + \mu/\lambda). \tag{1.36}$$

Putting $\mu = 1/L$, $c = 1/V$, and $\lambda = 1/A$ in equation (1.36), we obtain equation (32), which was discussed in the main text and more fully (but without derivation) in Anderson & May (1982). Similar results can clearly be found for type B and other survival functions.

The ratios \hat{w} and $\hat{\rho}$

As discussed in the main text, equation (35) gives the ratio, $\hat{w}(a_1, a_2)$, between the incidence of infection in the age range a_1 to a_2 after a vaccination programme is established and the corresponding incidence before vaccination. This definition of \hat{w} involves the age-specific numbers of susceptibles, $X(a)$ and $X'(a)$, and the forces of infection, λ and λ' , before and after vaccination, respectively. The above analysis has, however, established formulae for $X(a)$ and $X'(a)$, and for the relationships of λ and λ' to R_0 , under general assumptions about mortality and about the nature of the vaccination programme. Substitution of the appropriate formulae into equation (35) for $\hat{w}(a_1, a_2)$ thus leads to the results that are displayed in the various figures.

In particular, if a proportion p of all infants are immunized effectively at birth, we can substitute from equations (1.8) and (1.22) into equation (35), and thence for type B survival obtain the explicit equation (36) that is discussed in the main text. The corresponding expression for type A survival is

$$\hat{w}(a_1, a_2) = (1 - p) \frac{[\lambda'(\lambda + \mu)] [\exp(-(\lambda' + \mu)a_1) - \exp(-(\lambda' + \mu)a_2)]}{[\lambda(\lambda' + \mu)] [\exp(-(\lambda + \mu)a_1) - \exp(-(\lambda + \mu)a_2)]}. \tag{1.37}$$

These results, along with that for Gompertz or type C survival, are shown in Fig. 3.

As defined by equation (37), the risk ratio function, $\hat{\rho}(a_1, a_2)$, differs from $\hat{w}(a_1, a_2)$ only in the additional factor $m(a)$ in the integrands. Thus the computation of $\hat{\rho}$ is similar to, but a bit more complicated than, that of \hat{w} . One minor subtlety arises when calculating \hat{w} or $\hat{\rho}$ for the U.K. vaccination strategy against rubella, where a proportion p of girls only are vaccinated at age b : here the number of susceptibles in \hat{w} or $\hat{\rho}$ refers usually to girls, and therefore ‘ p ’ should be used; but in calculating the population-wide change in the force of infection, λ' , a factor ‘ $p/2$ ’ should be employed (as discussed following equation (1.32), above).

Maternal antibodies

As explained in the main text, the protection provided by maternal antibodies may be described by adding a further class, $I(a)$, of protected infants. In equations (1.1)–(1.5), equation (1.1) is then replaced by the two equations

$$dI/da = -(d + \mu(a))I(a), \tag{1.38}$$

$$dX/da = dI - (\lambda + \mu(a))X(a). \tag{1.39}$$

Integrating these equations, subject to the boundary conditions discussed in the main text, we get

$$I(a) = N(0) \exp(-da) \phi(a), \tag{1.40}$$

$$X(a) = N(0) [d/(d-\lambda)] [\exp(-\lambda a) - \exp(-da)] \phi(a). \tag{1.41}$$

For *type A survival*, equation (1.40) and (1.41) give equation (24) and (25) in the main text, and thence give Fig. 2.

The average age at infection, A , is given by equation (2.3) in Appendix 2, where $x(a) = X(a)/N(a)$ follows from equations (1.41) and (1.9). Thus

$$A = \int_0^\infty a [\exp(-\lambda a) - \exp(-da)] da / \int_0^\infty [\exp(-\lambda a) - \exp(-da)] da. \tag{1.42}$$

this gives equation (26) of the main text.

For *type A survival*, integration of equation (1.41) gives

$$\bar{X} = dN(0)/[(\lambda + \mu)(d + \mu)]. \tag{1.43}$$

With \bar{N} still given by equation (1.11), equation (12) now leads to the result

$$R_0 = (1 + \mu/d)(1 + \lambda/\mu). \tag{1.44}$$

Using $\mu = 1/L$, $d = 1/D$, and $\lambda = 1/(A - D)$ from equation (27), we arrive at equation (28), which is discussed in the main text.

For *type B survival*, the corresponding result is

$$\bar{X} = \{dN(0)/(d - \lambda)\} \{[1 - \exp(-\lambda L)]/\lambda - [1 - \exp(-dL)]/d\}. \tag{1.45}$$

If λL and dL are very large, as they usually are, this leads to the good approximation

$$\bar{X} \simeq N(0)/\lambda. \tag{1.46}$$

In conjunction with equation (1.15) for \bar{N} , equation (1.46) gives the approximate equation (30) for R_0 .

Dynamics of $\bar{X}(t)$, etc.

Under the assumptions that survival is of type A (μ constant), that births exactly balance deaths, and that λ is constant, we can integrate over all ages in equations (3)–(6), to get ordinary differential equations for the total number of susceptibles, $\bar{X}(t)$, defined by equation (1), and so on. If we further make the assumption of strong homogeneous mixing, equation (7), we arrive at a set of equations which have been much studied in the epidemiological literature:

$$d\bar{X}/dt = \mu\bar{N} - (\mu + \beta\bar{Y})\bar{X}, \tag{1.47}$$

$$d\bar{H}/dt = \beta\bar{Y}\bar{X} - (\sigma + \mu)\bar{H}, \tag{1.48}$$

$$d\bar{Y}/dt = \sigma\bar{H} - (\gamma + \mu)\bar{Y}, \tag{1.49}$$

$$d\bar{Z}/dt = \gamma\bar{Y} - \mu\bar{Z}, \tag{1.50}$$

$$d\bar{N}/dt = 0. \tag{1.51}$$

Consider first the situation where the population is wholly free of infection and everyone is susceptible, $\bar{X}(0) = \bar{N}$. If an infection is introduced, it will only be able

to increase if the right-hand sides of equations (1.48) and (1.49) are both positive, which requires $\beta\bar{Y}\bar{N} > (\sigma + \mu)\bar{H}$ and $\sigma\bar{H} > (\gamma + \mu)\bar{Y}$. This implies that the infection can 'take off' only if $\bar{N} > \bar{N}_T$, with \bar{N}_T defined by equation (16).

The equilibrium values of \bar{X} and other variables are obtained by setting the left-hand sides equal to zero in equations (1.47)–(1.50). It can then be seen that the equilibrium value of \bar{X} is \bar{N}_T , defined by equation (16), which again requires $\bar{N} > \bar{N}_T$ for the infection to persist at equilibrium (because $\bar{N} \geq \bar{X}$). Equation (12) with $\bar{X} = \bar{N}_T$ gives equation (14) or (15) for R_0 . Note that the structure of equations (1.47)–(1.51) is sufficiently straightforward for the same answers to emerge both from an equilibrium analysis and from considerations of the initial introduction of infection.

Dietz (1975) has shown how equation (20) for R_0 can be obtained directly from equations (1.47)–(1.51) and the definition of A (actually, Dietz's analysis does not include a latent class, but the essentials are there). We refer the reader to Dietz for this approach to the relations among R_0 , λ and A for type A survival.

APPENDIX 2

Methods for the estimation of the force of infection, λ , from data recording the age distribution of infection within populations were first described by Wilson & Worcester (1941) and Muench (1958). These methods are based on simple deterministic models, called 'catalytic models', which mimic the decay with age in the proportion of the population susceptible to infection. More recently Griffiths (1974) has considered certain statistical problems surrounding the use of these methods.

The epidemiological data on which such estimation procedures may be based can be either serological surveys or case notification records. Such information, stratified according to age, may be obtained from either horizontal or longitudinal epidemiological studies. Longitudinal studies, which follow the infection experiences of a given cohort of children all born in the same year, and which are based on serological survey, provide the most accurate information (provided of course the serological test is specific and sensitive). Case notification records are notoriously unreliable due to under-reporting, which may itself be a function of the age of the child. In practice, however, much of the available information is based on case notification records.

Model

Within an unvaccinated population of constant size \bar{N} in which the infection is at its endemic equilibrium, the number of individuals of age a who are susceptible to infection when exposed to a constant age-independent force of infection λ is given by equation (17) in the main text. The proportion susceptible at age a , $x(a) = X(a)/N(a)$, follows from equations (17) and (18) and is

$$x(a) = \exp(-\lambda a). \quad (2.1)$$

More generally, if the force of infection $\lambda(a)$ is age-dependent, then

$$x(a) = \exp\left[-\int_0^a \lambda(s) ds\right]. \quad (2.2)$$

The mean age at infection A is given by

$$A = \frac{\int_0^\infty a\lambda(a)x(a) da}{\int_0^\infty \lambda(a)x(a) da}. \tag{2.3}$$

Substituting equation (2.2) in equation (2.3), and performing a partial integration in the numerator, we obtain for A the equivalent formula

$$A = \int_0^\infty x(a) da. \tag{2.4}$$

The probability density function $g(a)$ for the age distribution in infection is thus given by

$$g(a) = x(a)/A, \tag{2.5}$$

and hence the average force of infection, $\bar{\lambda}$, is

$$\bar{\lambda} = \int_0^\infty \lambda(a)g(a) da = 1/A. \tag{2.6}$$

In other words, the average force of infection is equal to the reciprocal of the mean age at infection.

In much of the early use of the above models, the force of infection λ was assumed to be constant in value and independent of host age. Griffiths (1974), however, in an analysis of the age distribution of infection for measles in England and Wales, noted that λ tends to rise linearly with age between the ages of 0 and 10 years. Similar trends have been noted for other childhood infections in western societies (Anderson & May, 1982). For infections such as measles and pertussis, prior to wide-scale immunization, more than 95% of all cases occurred before the age of 10 years. One further aspect of the biology of the association between host and disease agent of importance in the estimation of λ is the duration of protection to infection in young infants provided by maternal antibodies. If we denote the average duration of protection by the symbol D , then a linear trend for λ to increase with age may be captured empirically by

$$\begin{aligned} \lambda(a) &= m + va \quad (a > D) \\ \lambda(a) &= 0 \quad (a \leq D) \end{aligned} \tag{2.7}$$

It follows from equations (2.2) and (2.5) that, for $a > D$, the proportion of individuals who have experienced the infection $q(a)$ is

$$q(a) = 1 - \exp \left[D \left(m + \frac{v}{2} D \right) - a \left(m + \frac{va}{2} \right) \right] \tag{2.8}$$

Calculation of $\lambda(a)$ from observed data

An estimation of λ in the time interval a to $(a + \Delta a)$ where Δa is small, may be obtained by means of equation (2.2) where

$$(a + \frac{1}{2}\Delta a) = -\ln \left[\frac{x(a + \Delta a)}{x(a)} \right] / \Delta a. \tag{2.9}$$

It is here assumed that λ is approximately constant in value over the small interval a to $a + \Delta a$. Given values of $x(a)$ it is possible to calculate the values of $\lambda(a)$ and to fit, by standard statistical procedures, a suitable empirical function to mirror the relationship between the force of infection and host age. Given $\lambda(a)$ the average age of infection, A , can be calculated by means of equation (2.3). To illustrate this procedure we provide below an example using case notification records for measles in England and Wales during the year 1977.

Table 2.1. *Case notifications by age of measles in England and Wales during 1977*

Age class (years)	Number of cases notified ($\hat{Y}(a)$)	Proportion susceptible ($x(a)$)	Age, a (years) (midpoint of age class)	$\lambda(a)$
0.5-1	16508	0.969	0.75	0.0629
1-2	50331	0.875	1.5	0.1024
2-3	65003	0.753	2.5	0.1500
3-4	69132	0.623	3.5	0.1900
4-5	71283	0.490	4.5	0.2413
5-10	246041	0.028	7.5	0.5686
10-15	15216	0.000	12.5	—
Total	533514			

The proportion of susceptibles $x(a)$ in Table 2.1 is formally defined as

$$x(a) = \left[1 - \frac{\int_0^a \lambda(s) X(s) ds}{\int_0^\infty \lambda(s) X(s) ds} \right], \quad (2.10)$$

where $\hat{Y}(a) = \lambda(a) X(a)$. If we assume that the vast majority of the cases occur by the age of 15 years then equation (2.10) may be approximated by

$$x(a) = \left[1 - \frac{\sum_0^a \hat{Y}(a)}{\sum_0^{15} \hat{Y}(a)} \right]. \quad (2.11)$$

The values for $\lambda(a)$ recorded in the last column of Table 2.1 are calculated by means of equation (2.9). The estimated values for $x(a)$ recorded in the middle column of the table are calculated on the assumptions: (a) that there is no age-related bias in the degree of under-reporting; (b) that the disease is at its endemic equilibrium such that the horizontal picture of age-related notifications reflects longitudinal trends; and (c) that virtually all cases of measles occur in the first 15 years of life (for 1977 99% occurred in the age classes 0-15). Assumption (c) is satisfied but (a) and (b) are unlikely to be so. Cyclical trends in disease incidence will tend to invalidate assumption (b), but provided these cycles are short (i.e. 2 years for measles) in relation to the age span examined (i.e. 0-15 years of age) this source of error is unlikely to be serious. Assumption (a) is the most difficult to test, since detailed quantitative data on this aspect of case reporting is not in general available. However, it must be recognized as a potential source of error.

Given these caveats, the linear model defined in equation (2.7) for $\lambda(a)$ can be fitted to the data recorded in the last two columns of Table 2.1 by standard statistical procedures. This yields the parameter estimates (given $D = 0.5$ years) $m = -0.0275$ and $v = 0.0730$ with a correlation coefficient r for the goodness of fit of the linear model of 0.97. By means of numerical integration procedures equation (2.3) may be solved, given estimates of the parameters D , m and v , to provide an estimate of A , the average age at infection. The calculated value for the data recorded in Table 2.1 is $A = 5.0$ years.

APPENDIX 3

In this appendix we discuss a very simple model for the dynamics of infection; this model helps us to understand the propensity for the incidence of infection to exhibit cyclic oscillations, with period given approximately by equation (31). Our simple model has previously been discussed by Fine & Clarkson (1982*b*), although their study does not bring out the oscillatory features (also, we give explicit form to quantities that they treat as general parameters). The relation of our model to others used in dynamical studies of infection is discussed below.

The model treats the dynamical variables as changing in discrete time steps, an interval τ apart. Usually, τ will be the average time between an individual acquiring infection and passing it on to a subsequent infectee; that is, τ is usually equal to the quantity K defined in equation (31), $\tau = K = 1/\sigma + 1/\gamma$. Ignoring any latent period, we define the total number of susceptibles to be S_t , and the total number of infectious individuals (or cases) to be C_t , at time t . One time step τ later, the number of cases will be

$$C_{t+\tau} = (R_0 S_t / N) C_t. \tag{3.1}$$

Here each case at time t produces R_0 secondary cases at time $t + \tau$ if the entire population is susceptible, or $R_0 S_t / N$ if only the fraction S_t / N is susceptible. The number of susceptibles at $t + \tau$ is equal to S_t augmented by births (assuming all are born susceptible) and diminished by the new cases

$$S_{t+\tau} = S_t - C_{t+\tau} + B. \tag{3.2}$$

Net births, B , in the time interval τ are equal to $\mu\tau N$, where μN is the total annual birthrate (assuming a steady-state population).

The equilibrium solution of equations (3.1) and (3.2) is found by putting $S_{t+\tau} = S_t = S^*$ and $C_{t+\tau} = C_t = C^*$, to get

$$C^* = B = \mu\tau N, \tag{3.3}$$

and

$$S^* = N / R_0. \tag{3.4}$$

The local stability of this equilibrium point can be studied by standard techniques, discussed elsewhere (e.g. May, 1974); what follows is a sketchy outline. We write $S_t = S^* + s_t$, $C_t = C^* + c_t$, and neglect terms of second or higher order in s_t and c_t in the Taylor expanded version of equations (3.1) and (3.2):

$$c_{t+\tau} = c_t + (R_0 B / N) s_t, \tag{3.5}$$

$$s_{t+\tau} = s_t - c_{t+\tau}. \tag{3.6}$$

This pair of linear equations can now be solved by factoring out the time dependence in the eigenvalue Λ , where $s_t \sim s_0 \Lambda^n$, $c_t \sim c_0 \Lambda^n$ with $n = t/\tau$ being the number of time steps from 0 to t . Thus defined, Λ satisfies the quadratic equation

$$\Lambda^2 - 2(1 - \epsilon)\Lambda + 1 = 0. \quad (3.7)$$

Here ϵ has been defined for notational convenience as

$$\epsilon = \frac{1}{2}R_0 B/N = \frac{1}{2}\mu R_0 \tau. \quad (3.8)$$

It follows that

$$\Lambda = (1 - \epsilon) \pm i[1 - (1 - \epsilon)^2]^{\frac{1}{2}}. \quad (3.9)$$

That is, Λ is a complex number with modulus unity; Λ can be rewritten as

$$\Lambda = \exp(i\theta\tau) \quad (3.10)$$

with

$$\theta \equiv [\cos^{-1}(1 - \epsilon)]/\tau. \quad (3.11)$$

That is to say, the time dependence of the perturbations s_t and c_t is characterized by the behaviour of the function $\Lambda^{t/\tau}$,

$$s_t, c_t \sim \exp(i\theta t). \quad (3.12)$$

Since the magnitude of the eigenvalue Λ is unity, a small disturbance to the equilibrium state given by equations (3.3) and (3.4) simply oscillates indefinitely, exhibiting the neutral stability of the frictionless pendulum (for a more detailed discussion of neutral stability, see May, 1974). The period, T , of these continuing oscillations is given immediately from equation (3.12):

$$T = 2\pi/\theta. \quad (3.13)$$

Finally, we remark that the approximate but rather general equation (23) says that $\mu R_0 \simeq 1/A$, so that $\epsilon \simeq \tau/2A$. the quantity ϵ is thus small, unless τ is of order A (which it certainly never will be if τ is K), and so a good approximation in equation (3.11) is

$$\theta \simeq (2\epsilon)^{\frac{1}{2}}/\tau \simeq (A\tau)^{-\frac{1}{2}}. \quad (3.14)$$

Thus we have neutrally stable oscillations with period T approximately given by

$$T \simeq 2\pi(A\tau)^{\frac{1}{2}}. \quad (3.15)$$

This is exactly equation (31) in the natural and usual case where $\tau = K$, as discussed in the main text.

The model used in Soper's (1929) classic study was, in essentials, a continuous time version of that above. Such differential equations are more stable than the corresponding difference equations, and so Soper found damped – but weakly damped – oscillations with the above period. Bartlett studied a model with a difference equation similar to that above, with a slight modification that tipped the stability towards damping, but also with stochastic elements that give the net result of sustained oscillations at approximately the above period. The variety of more recent studies cited in the main text are all, in their essentials, studies of the above model, with various refinements that contend to tip the system either to

damped oscillations or to sustained stable-limit cycles, in either case with periods given by equation (31).

Knox's (1980) studies of the dynamical behaviour of the incidence of rubella, following the introduction of specific vaccination programmes, use a model that is basically equations (3.1) and (3.2), but with a time step τ of one year. He consequently finds a propensity for the system to oscillate, with a period set by equation (3.15). By taking $\tau = 1$ year (instead of the more accurate $\tau = K$, where K for rubella is around 2–3 weeks), Knox gets a basic time scale (and period) that we believe to be too long by the factor $(1/K)^{\frac{1}{2}}$, or around a factor 5.

APPENDIX 4

Within the framework of the model defined by equations (3)–(6), the changes in the number of susceptibles of age a at time t , $X(a, t)$, following the introduction of a vaccination programme at time $t = 0$, are given by

$$\partial X/\partial t + \partial X/\partial a = -[\lambda(t) + c(a) + \mu(a)]X(a, t). \tag{4.1}$$

The initial value $X(a, 0)$ at $t = 0$ is the pre-vaccination equilibrium distribution described by equation (17), and $X(0, t) = N(0)$, the number of births, for all t . Here, as previously discussed, we have assumed that births exactly balance deaths, that the force of infection is independent of age, and that the age-specific vaccination programme does not vary over time (so that c is $c(a)$, which is, at best, only approximately true for real programmes).

Equation (4.1) can be integrated, to get the explicit solution for $t > 0$:

$$X(a, t) = N(0) \exp(-\psi(a, t)). \tag{4.2}$$

Here ψ is defined as

$$\psi(a, t) = \int_0^a \mu(s) ds + \int_{a-t}^a c(s) ds + \int_{t-a}^t \lambda(s) ds. \tag{4.3}$$

In the integrations in this equation (4.3), it is to be understood that $c(s) = 0$ for $s < 0$, and that $\lambda(s) = \lambda_0$ for $s < 0$, with λ_0 the force of infection at equilibrium in the initial, pre-vaccination population (as given, for example, by equation (21) for type B survival). This result can be derived by using the 'method of characteristics' (see, e.g., Hoppensteadt, 1974), which is essentially a mathematical consequence of the biological fact that as time t passes an individual's age advances from a to $a + t$. Those who are not happy with this terse statement can check equations (4.2) and (4.3) by verifying that they indeed satisfy the partial differential equation (4.1), along with the initial and boundary conditions.

In the special case where the programme consists of vaccinating a proportion p at birth, the above results reduce to

$$X(a, t) = N(0) \phi(a) \exp\left[-\lambda_0(a-t) - \int_0^t \lambda(s) ds\right] \quad (\text{for } 0 \leq t < a) \tag{4.4a}$$

$$X(a, t) = (1-p) N(0) \phi(a) \exp\left[-\int_{t-a}^t \lambda(s) ds\right] \quad (\text{for } t > a) \tag{4.4b}$$

Here the mortality factor is contained in the function $\phi(a)$ defined by equation (1.7).

More generally, if a proportion p are vaccinated at exactly age b , we get the following results. For $a > t$ and either $a \leq b$ or $a > t + b$,

$$X(a, t) = N(0) \phi(a) \exp \left[-\lambda_0(a-t) - \int_0^t \lambda(s) ds \right]. \tag{4.5a}$$

For $a > t > a - b > 0$,

$$X(a, t) = (1-p) N(0) \phi(a) \exp \left[-\lambda_0(a-t) - \int_0^t \lambda(s) ds \right]. \tag{4.5b}$$

For larger t , $t > a$, we get

$$X(a, t) = N(0) \phi(a) \exp \left[-\int_{t-a}^t \lambda(s) ds \right] \quad (\text{for } a \leq b), \tag{4.5c}$$

$$X(a, t) = (1-p) N(0) \phi(a) \exp \left[-\int_{t-a}^t \lambda(s) ds \right] \quad (\text{for } a > b). \tag{4.5d}$$

This result, equation (4.5), reduces to equation (4.4) in the limit $b \rightarrow 0$, as it should. It is also reassuring to notice that, in the limit $t \rightarrow \infty$ (where $\lambda(t) \rightarrow \lambda'$), equation (4.4) reduces asymptotically to the post-vaccination equilibrium result equation (1.22), and equation (4.5) to the corresponding equation (1.28).

The above formulae give $X(a, t)$ in terms of known quantities and $\lambda(t)$. We can, however, no longer use the equilibrium equation (12) to determine λ (as was done throughout Appendix 1). Instead, we relate $\lambda(t)$ to $\bar{Y}(t)$ by equation (7), $\lambda(t) = \beta \bar{Y}(t)$, which was discussed in the main text. We now obtain three ordinary differential equations for $\lambda(t)$, $\bar{X}(t)$ and $\bar{H}(t)$, for the special case where a proportion p of susceptibles are vaccinated at age b ; vaccination of a proportion p at birth follows as the limit $b \rightarrow 0$. This special case is the basis for all our dynamical studies (sometimes with ' p ' replaced by ' $p/2$ ', when only girls are vaccinated, as discussed in the main text).

For *type A survival*, as is usually assumed in such studies, we can integrate equation (4.1) over all ages to get the ordinary differential equation

$$d\bar{X}/dt = -(\lambda(t) + \mu) \bar{X}(t) + X(0, t) - pX(b, t). \tag{4.6}$$

In equation (4.6), $X(0, t) = N(0)$ as always, and $X(b, t)$ is given by equation (4.5a) or (4.5c). The remaining two ordinary differential equations that close the system are equations (1.48) and (1.49) of Appendix 1, with $\lambda(t)$ replacing $\beta \bar{Y}(t)$ throughout.

Our actual calculations, however, are all based on the more realistic *type B survival*. Integration of equation (4.1) over all ages $0-L$ (where $\mu = 0$) gives

$$d\bar{X}/dt = -\lambda(t) \bar{X}(t) + X(0, t) - pX(b, t) - X(L, t); \tag{4.7}$$

again, $X(b, t)$ and $X(L, t)$ are given by equation (4.5a) or (4.5c). The corresponding differential equations for $\bar{H}(t)$ and $\lambda(t)$ are

$$d\bar{H}/dt = \lambda(t) \bar{X}(t) - \sigma \bar{H}(t) - H(L, t), \tag{4.8}$$

$$d\lambda/dt = \beta \sigma \bar{H}(t) - \gamma \lambda(t) - \beta Y(L, t). \tag{4.9}$$

The quantity $H(L, t)$ will be of order $\bar{H}(t)/L$, and thus will be smaller than $\sigma \bar{H}(t)$

by a factor of order $1/(\sigma L)$, which is the ratio between the duration of the latent period and the life expectancy; since $1/\sigma$ is of the order of days, and L is of the order of decades, the term $H(L, t)$ may usually, to an excellent approximation, be neglected. Similarly, the ratio of $Y(L, t)$ to $\gamma \bar{Y}(t)$ is of order $1/(\gamma L)$, which likewise is very small.

When the terms $H(L, t)$ and $Y(L, t)$ are omitted, equations (4.7)–(4.9) give a set of three nonlinear differential equations, which can be integrated numerically (the initial conditions are supplied by the pre-vaccination equilibrium values of \bar{X} , \bar{H} and λ_0). In this way we compute the dynamical trajectories of $\lambda(t)$ and $X(a, t)$, and thence of the non-equilibrium ratios $w(a_1, a_2; t)$ and $\rho(a_1, a_2; t)$, that are presented and discussed in the main text.

The same results can, of course, be obtained directly by numerical solution of the partial differential equations (3)–(6), and this can be necessary for more complicated vaccination strategies (particularly if $c(a, t)$ is changing over time). Conversely, the analytic approach developed above can be carried further, to get a good basic understanding of how the dynamical behaviour works; such display of mathematical virtuosity will be presented elsewhere.

REFERENCES

- ANDERSON, R. M. & MAY, R. M. (1982). Directly transmitted infectious diseases: control by vaccination. *Science* **215**, 1053–60.
- ARON, J. L. (1983). A stochastic model of infection boosted by re-infection. In preparation.
- ARON, J. L. & SCHWARTZ, I. B. (1983). Seasonality and period doubling bifurcations in an epidemic model. *Journal of Theoretical Biology* (In the Press.)
- BAILEY, N. T. J. (1975). *The Mathematical Theory of Infectious Diseases and its Applications*. London: Griffin.
- BARTLETT, M. S. (1957). Measles periodicity and community size. *Journal of the Royal Statistical Society, A* **120**, 48–70.
- BARTLETT, M. S. (1960). The critical community size for measles in the United States. *Journal of the Royal Statistical Society, B*, **123**, 37–44.
- BECKER, N. (1979). The uses of epidemic models. *Biometrics*, **35**, 295–305.
- BENENSON, A. S. (1975). *Control of Communicable Diseases in Man*, 12th ed. Washington, D.C.: American Public Health Association.
- BLACK, F. L. (1966). Measles endemicity in insular populations: critical community size and its evolutionary implications. *Journal of Theoretical Biology* **11**, 207–211.
- CENTER FOR DISEASE CONTROL (1981a). Rubella—United States, 1978–1981. *Morbidity and Mortality Weekly Report* **30**, 513–515.
- CENTER FOR DISEASE CONTROL (1981b). Measles encephalitis—United States 1962–1979. *Morbidity and Mortality Weekly Report* **31**, 217–224.
- CENTER FOR DISEASE CONTROL (1982a). Measles prevention. *Morbidity and Mortality Weekly Report* **31**, 217–224.
- CENTER FOR DISEASE CONTROL (1982b). Measles—El Paso, Texas, 1981. *Morbidity and Mortality Weekly Report* **31**, 182–183.
- CENTER FOR DISEASE CONTROL (1982c). School immunization requirements for measles—United States, 1982. *Morbidity and Mortality Weekly Report* **31**, 65–67.
- CENTER FOR DISEASE CONTROL (1982d). Measles—United States, first 26 weeks, 1982. *Morbidity and Mortality Weekly Report* **31**, 381–382.
- CLARKE, M., SCHILD, G. C., BOUSTRED, J., MCGREGOR, I. A. & WILLIAMS, K. (1980). Epidemiological studies of rubella virus in a tropical African community. *Bulletin of the World Health Organisation* **58**, 931–935.
- CLARKE, M., SCHILD, G. C., BOUSTRED, J., SEAGROATT, V., POLLOCK, T. M., FINDLAY, S. E. & BARBARA, J. A. J. (1979). Effect of rubella vaccination programme on the serological states of young adults in the U.K. *Lancet* **i**, 1224.

- COLLINS, S. D. (1929). Age incidence of the common communicable diseases of children. *United States Public Health Reports* **44**, 763–828.
- CVJETANOVIC, B., GRAB, B. & DIXON, H. (1982). Epidemiological models of poliomyelitis and measles and their application in the planning of immunization programmes. *Bulletin of the World Health Organisation* **60**, 405–422.
- DAVIS, R. (1982). Measles in the tropics and public health practices. *Transactions of the Royal Society of Tropical Medicine and Hygiene* **76**, 268–275.
- DIETZ, K. (1975). Transmission and control of arbovirus diseases. In *Epidemiology* (ed. D. Ludwig and K. L. Cooke), pp. 104–121. Philadelphia: Society for Industrial and Applied Mathematics.
- DIETZ, K. (1976). The incidence of infectious diseases under the influence of seasonal fluctuations. *Lecture Notes in Biomathematics* **11**, 1–15.
- DIETZ, K. (1981). The evaluation of rubella vaccination strategies. In *The Mathematical Theory of the Dynamics of Biological Populations*, vol. II (ed. R. W. Hiorns and D. Cooke), pp. 81–98. London: Academic Press.
- DIETZ, K. (1982). Overall population patterns in the transmission cycle of infectious disease agents. In *Population Biology of Infectious Disease* (ed. R. M. Anderson and R. M. May), pp. 87–102.
- EDMOND, E., MORTON, P., MOFFAT, M. & URQUHART, G. E. D. (1980). *Health Bulletin* **38**, 54.
- FINE, P. E. M. & CLARKSON, J. (1982a). Measles in England and Wales. I. An analysis of the factors underlying seasonal patterns. *International Journal of Epidemiology* **11**, 5–14.
- FINE, P. E. M. & CLARKSON, J. E. (1982b). Measles in England and Wales. II. The impact of the measles vaccination programme on the distribution of immunity in the population. *International Journal of Epidemiology* **11**, 15–25.
- FINE, P. E. M. & CLARKSON, J. A. (1983). Measles in England and Wales. III. Assessing published predictions of the impact of vaccination on incidence. *International Journal of Epidemiology*. (In the Press.)
- FISHER, R. A. (1930). *The Genetical Theory of Natural Selection*. New York: Dover (reprint, 1958).
- FOX, J. P., ELVEBACK, L., SCOTT, W., GALEWOOD, L. & ACKERMAN, E. (1971). Herd immunity: basic concept and relevance to public health immunization practices. *American Journal of Epidemiology* **94**, 179–189.
- GREGG, N. M. (1941). Congenital cataract following German measles in the mother. *Transactions of the Ophthalmic Society of Australia* **3**, 35.
- GRIFFITHS, D. A. (1974). A catalytic model of infection for measles. *Applied Statistics* **23**, 330–339.
- GRIST, N. R., REID, D. & YOUNG, A. B. (1981). Herd immunity to infections. *Health Bulletin* **39**, 211–217.
- GROSSMAN, Z. (1980). Oscillatory phenomena in a model of infectious diseases. *Theoretical Population Biology* **18**, 204–243.
- HANSHAW, J. B. & DUDGEON, J. A. (1978). *Viral Diseases of the Fetus and Newborn*. W. B. Saunders Company, London.
- HAYDON, G. F., MODLIN, J. F. & WITTLE, J. J. (1977). Current status of rubella in the United States 1969–75. *Journal of Infectious Diseases* **185**, 337–340.
- HETHCOTE, H. W. (1978). An immunization model for the heterogeneous population. *Theoretical Population Biology* **14**, 338–349.
- HETHCOTE, H. W. (1983). Measles and rubella in the United States. *American Journal of Epidemiology*. (In the Press.)
- HETHCOTE, H. W., STECH, H. W. & VAN DEN DRIESCHE, P. (1981). Nonlinear oscillations in epidemic models. *SIAM Journal of Applied Mathematics* **40**, 1–9.
- HETHCOTE, H. W. & TUDOR, D. W. (1980). Integral equation models for endemic infectious diseases. *Journal of Mathematical Biology* **9**, 37–47.
- H.M.S.O. (1981). *Whooping Cough*. London: Her Majesty's Stationery Office.
- HOPPENSTEADT, F. C. (1974). An age dependent epidemic model. *Journal of the Franklin Institute* **297**, 325–333.
- HOPPENSTEADT, F. C. (1975). *Mathematical Theories of Populations: Demographics, Genetics and Epidemics*. Philadelphia: SIAM (Regional Conference Series in Applied Mathematics, 20).
- KERMACK, W. O. & MCKENDRICK, A. G. (1927). A contribution to the mathematical theory of epidemics. *Proceedings of the Royal Society A* **115**, 13–23.
- KNOX, E. G. (1980). Strategy for rubella vaccination. *International Journal for Epidemiology* **9**, 13–23.

- MACDONALD, G. (1952). The analysis of equilibrium in malaria. *Tropical Diseases Bulletin* **49**, 813–829.
- MCCARTNEY, A. & ROSS, C. A. C. (1979). *Communicable Diseases, Scotland Weekly Report* No. 15.
- MAY, R. M. (1974). *Stability and Complexity in Model Ecosystems*, 2nd ed. Princeton: Princeton University Press.
- MORLEY, D. C. (1969). Severe measles in the tropics. 1. *British Medical Journal* **i**, 293–300.
- MUENCH, H. (1959). *Catalytic Models in Epidemiology*. Cambridge, Mass.: Harvard University Press.
- NOLD, A. (1979). The infectee number at equilibrium for a communicable disease. *Mathematical Biosciences* **46**, 131–138.
- PREBLUD, S. R., SERDULA, M. K., FRANK, J. A. JR., BRANDLING-BENNETT, A. D. & HINMAN, A. R. (1980). Rubella vaccination in the United States: a ten year review. *Epidemiological Reviews* **2**, 171–194.
- SMITH, H. L. (1983). Multiple stable subharmonics for a periodic epidemic model. (Preprint.)
- SOPER, H. E. (1929). Interpretation of periodicity in disease prevalence. *Journal of the Royal Statistical Society* **92**, 34–73.
- STARR, C. & WHIPPLE, C. (1980). Risks of risk decisions. *Science* **208**, 1114–1119.
- URQUHART, G. E. D. (1980). *Communicable Diseases Scotland Weekly Report* No. 24.
- WALTMAN, P. (1974). *Deterministic Threshold Models in the Theory of Epidemics* (Lecture Notes in Biomathematics). New York: Springer-Verlag.
- WICKWIRE, K. (1977). Mathematical models for the control of pests and infectious diseases: a survey. *Theoretical Population Biology* **11**, 182–238.
- WILSON, E. B. & WORCESTER, J. (1941). Contact with measles. *Proceedings of the National Academy of Sciences, Washington* **27**, 7–13.
- YORKE, J. A., NATHANSON, N., PIANINGIANI, G. & MARTIN, J. (1979). Seasonality and the requirements for perpetuation and eradication of viruses. *American Journal of Epidemiology* **109**, 103–123.